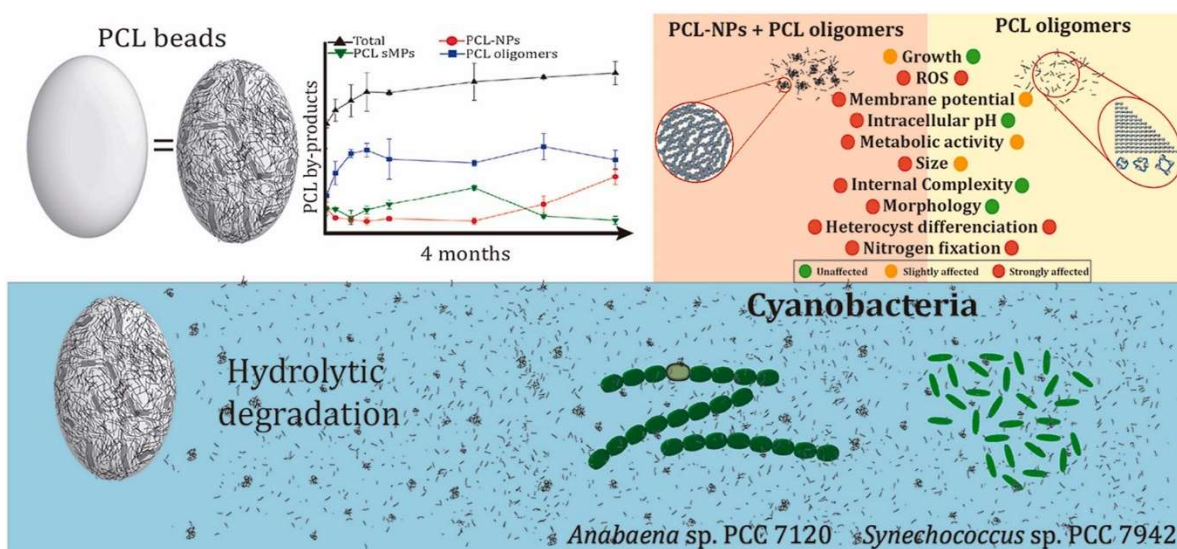# Identification and toxicity towards aquatic primary producers of the smallest fractions released from hydrolytic degradation of polycaprolactone microplastics

Identification and toxicity towards aquatic primary producers of the smallest fractions released from hydrolytic degradation of polycaprolactone microplastics

Miguel Tamayo-Belda[1], Gerardo Pulido-Reyes[1], Miguel González-Pleiter[1], Keila Martín-Betancor[1], Francisco Leganés[1], Roberto Rosal[2], FranciscaFernández-Piñas[1,*]

[1] Department of Biology, Faculty of Science, Universidad Autónoma de Madrid, E-28049, Madrid, Spain

[2] Department of Chemical Engineering, Universidad de Alcalá, 28805 Alcalá de Henares, Madrid, Spain

* Corresponding author: francisca.pina@uam.es

Abstract

Bioplastics are thought as a safe substitute of non-biodegradable polymers. However, once released in the environment, biodegradation may be very slow, and they also suffer abiotic fragmentation processes, which may give rise to different fractions of polymer sizes. We present novel data on abiotic hydrolytic degradation of polycaprolactone (PCL), tracking the presence of by-products during 132 days by combining different physicochemical techniques. During the study a considerable amount of two small size plastic fractions were found (up to ~ 6 mg of PCL by-product/g of PCL beads after 132 days of degradation); and classified as submicron-plastics (sMPs) from 1 μm to 100 nm and nanoplastics (NPs, <100 nm) as well as oligomers. The potential toxicity of the smallest fractions, PCL by-products < 100 nm (PCL-NPs + PCL oligomers) and the PCL oligomers single fraction, was tested on two ecologically relevant aquatic primary producers: the heterocystous filamentous nitrogen-fixing cyanobacterium *Anabaena* sp. PCC 7120, and the unicellular cyanobacterium *Synechococcus* sp. PCC 7942. Upon exposure to both, single and combined fractions, Reactive Oxygen Species (ROS) overproduction, intracellular pH and metabolic activity alterations were observed in both organisms, whilst membrane potential and morphological damages were only observed upon PCL-NPs + PCL oligomers exposure. Notably both PCL by-products fractions inhibited nitrogen fixation in *Anabaena*, which may be clearly detrimental for the aquatic trophic chain. As conclusion, fragmentation of bioplastics may render a continuous production of secondary nanoplastics as well as oligomers that might be toxic to the surrounding biota; both PCL-NPs and PCL oligomers, but largely the nanoparticulate fraction, were harmful for the two aquatic primary producers. Efforts should be made to thoroughly understand the fragmentation of bioplastics and the toxicity of the smallest fractions resulting from that degradation.

Keywords: Bioplastics; PCL degradation; Nanoplastics; Oligomers; Toxicity; Cyanobacteria

1. Introduction

One of the main concerns about the widespread presence of plastic debris in the environment is their persistence (Lewis and Maslin, 1964). During the last 70 years, plastic production has overcome 9000 million tons, of which more than 70% ends up in landfills or directly in the environment (Geyer, 2020). The fragmentation and degradation of plastic occurs due to the environmental stressors that induce hydrolysis, photodegradation, thermo-oxidative degradation, mechanical abrasion and biodegradation (Mattsson et al., 2018). This way, plastics are broken down into smaller pieces, known as microplastics and nanoplastics (Hartmann et al., 2019). Nevertheless, the low reactivity and high stability of the carbon backbone of the most common polymers such as polyethylene (PE), polypropylene (PP), polyvinylchloride (PVC), polystyrene (PS) or polyethylene terephthalate (PET) result in extremely slow degradation rates (Chamas et al., 2020). Thereby, the unbalance between the plastic waste input and their complete degradation causes the accumulation in the environment. Which leads to a constant increase in the concentration of plastic particles, free oligomers, and additives (Eriksen et al., 2014; Groh et al., 2019).

Biodegradable polymers emerged as a sustainable alternative aimed to deal with plastic waste accumulation in the environment. Based on this approach, plastics should be designed to be extensively degradable both by abiotic and biotic agents, referred as "environmental degradation", in short periods of time (Huang et al., 1990). Despite its definition clearly pointing out the key role of the degrading organisms and cognate enzymes, the process still currently requires a previous fragmentation and scission of the high molecular weight chains by abiotic factors like hydrolysis (Degli-Innocenti, 2014; Obayashi and Kinoshita, 2009) (Agarwal, 2020; Degli-Innocenti, 2014). Nowadays, 2.42 million tonnes of plastics are produced per year. It is expected to increase to approximately 6.72 million tonnes in 2025 (European Bioplastics, 2021). Bioplastics are classified in three categories: biobased or partially biobased but non-biodegradable, such as biobased PE, PP, or PET; both

biobased and biodegradable, such as polylactic acid (PLA) or polyhydroxybutyrate (PHB); and based on fossil resources but biodegradable, such as polybutylene adipate terephthalate (PBAT) and polycaprolactone (PCL) (Picó and Barceló, 2019). Since biodegradation is determined not only by polymer characteristics but also by environmental factors such as the availability of oxygen and light, pH, temperature, or type of microorganisms present, the same bioplastic may show different degradation rates under different environmental conditions. Therefore, the biodegradability of the polymers classified as biodegradable cannot be taken as a direct measure of their fate under any environmental conditions. Accordingly, improper disposal management would result in an inefficient and uncontrolled biodegradation, thereby increasing existing plastic pollution (Agarwal, 2020; RameshKumar et al., 2020). The validation of bioplastics as sustainable alternative for the traditional oil-based plastics requires not only biodegradation studies and accurate classification but also toxicity assessment throughout their entire life cycle (Shen et al., 2020). Plastic debris poses a threat to the biota mainly due to three types of effects: direct contact with plastic particles, the release of co-transported pollutants, and the leaching of backbone oligomers or additives (Iñiguez et al., 2017). In this regard, only a few publications have studied the toxicological effects that might arise due to the uncontrolled disposal of biodegradable plastics. Several negative effects toward environmentally relevant organisms have been described for biodegradable microplastics (MPs); Green et al. (2016) exposed intact sediment cores containing European flat oysters (*Ostrea edulis*) or blue mussels (*Mytilus edulis*) in seawater to biodegradable or conventional MPs in outdoor mesocosms. This was done with the objective to test whether microplastics affected the filtration rates of the bivalves and other factors such as invertebrate community assemblage. Both types of MPs affected filtration by *M. edulis* but no effects were observed for ecosystem functioning or the associated invertebrates community. On the contrary, filtration by the oyster significantly increased when exposed to microplastics. In addition, the associated faunal assemblages differed. Their findings shed light on the potential of microplastics to affect the functioning and structure of sedimentary habitats. González-Pleiter et al. (2019) demonstrated that secondary PHB-nanoplastics were produced from PHB-MPs by abiotic degradation under environmentally representative conditions. These secondary PHB-nanoplastics induced a significant decrease in cellular growth and altered relevant physiological parameters in three model aquatic organisms: the cyanobacterium *Anabaena* sp. PCC7120, the green alga *Chlamydomonas reinhardtii* and the small crustacean *Daphnia magna*. Zimmermann et al. (2020) made extracts of 43 everyday bio-based and/or biodegradable products as well as their precursors and characterized these extracts using in vitro bioassays. They found that

two-third (67%) of the samples induced baseline toxicity, 42% oxidative stress, 23% antiandrogenicity and 1 sample estrogenicity. Raw materials were less toxic than their final products. A comparison with conventional plastics indicated that bioplastics and plant-based materials were similarly toxic. These findings highlight that biodegradable plastics may not be harmless for the biota, implying that biodegradable does not always mean safe and that chemical safety should be considered when designing truly safer plastic alternatives.

The global production and consumption of biodegradable plastics is led by thermoplastic starch blends and PLA (European Bioplastics, 2021). Nevertheless, PCL is widely used for biomedical applications such as medical devices, tissue engineering or drug delivery, either alone or blended (Raina et al., 2021). There are several studies that have tackled the use of PCL in preparing micro- and nanoparticles for controlled drug delivery given its high permeability to different drugs, excellent biocompatibility, and complete excretion from the body once used (Ali Akbari Ghavimi et al., 2015; Song et al., 2018). In the agriculture field, it has been also highlighted as potential nanocarrier of herbicides and fertilizers (Cesari et al., 2020; Diyanat et al., 2019; Pouladchang et al., 2022). Furthermore, PCL has been pointed out as an excellent copolymer together with PLA for home-compostable goods, even degradable under unmanaged environmental conditions (Havstad, 1994; Narancic et al., 2020). There is extensive literature regarding the molecular mechanisms involved in the degradation of PCL, which considers the role of the polymer structure and shape, radical interactions, pH, temperature, enzymatic activity, and cellular phagocytosis (Abriata et al., 2019; Al Hosni et al., 2019; Bartnikowski et al., 2019; Bosworth and Downes, 2010; Jarrett et al., 1984; Kasuya et al., 1998; Krasowska et al., 2016; Lam et al., 2008, 2009; Persenaire et al., 2001; Rivas et al., 2016; Woodward et al., 1985). From them, it can be concluded that PCL undergoes a two-stage degradation process: firstly, the hydrolytic cleavage of ester groups without enzymatic intervention, and, secondly, the biological degradation when the polymer has higher crystallinity and has a low molecular weight (Azimi et al., 2014). During both stages, PCL by-products are released, which are expected to interact with the surrounding organisms. However, their toxicological behavior remains scarcely studied in soils (Irizar et al., 2018), whilst in aquatic environments, to the best of our knowledge, it still remains understudied.

In this work, we aimed to test the hypothesis whether the hydrolytic degradation of plastics, including bioplastics such as PCL, will cause fragmentation of the polymer, and in the long term the release of different fractions of polymer sizes, including secondary nanoplastics and even oligomers in the water column that could be toxic for the surrounding biota. To achieve that, the presence and concentration of the

particulates and oligomeric fractions of PCL by-products was tracked during 132 days of hydrolytic degradation. Dry weight, total organic carbon, electrophoretic light scattering, single-angle and multi-angle dynamic light scattering, scanning electron microscopy, MALDI TOF/TOF and micro-Fourier transformation infra-red techniques were used. Additionally, the toxicity levels of the by-products released during the first 2 weeks of hydrolytic degradation were studied on two ecologically relevant aquatic primary producers, the heterocystous filamentous nitrogen-fixing cyanobacterium *Anabaena* sp. PCC 7120, (hereinafter *Anabaena*) and the unicellular cyanobacterium *Synechococcus* sp. PCC 7942, (hereinafter *Synechococcus*). Cyanobacteria represent an important fraction in the phytoplankton group; these organisms are at the base of the trophic web of aquatic ecosystems; therefore, any deleterious effect on them may also impair higher trophic level organisms, disrupting the ecological balance in the aquatic environments. In addition, they have been regularly used as model organisms for ecotoxicological studies (Gonzalo et al., 2015; Pulido-Reyes et al., 2015; Zhang et al., 2018; Tamayo-Belda et al., 2019; González-Pleiter et al., 2019; Feng et al., 2019). The toxicity endpoints included potential growth inhibition as well as the study of mechanisms of toxic action by studying overproduction of Reactive Oxygen Species (ROS), which may ultimately lead to oxidative stress and potential alterations in cytoplasmatic membrane potential, intracellular pH, non-specific esterase activity and morphology. In addition, given the importance of N_2 fixation in the aquatic ecosystems, the potential alteration of heterocyst differentiation (specialized cell for N_2 fixation under aerobiosis) and nitrogenase activity of *Anabaena* has been studied (Kumar et al., 2010).

2. Materials and methods

2.1. Chemicals

White to translucent beads of 3 mm diameter, density 1.145 g cm^{-3}, average Mn 80000 and Mw/Mn < 2) of PCL (impurities < 0.5% water) were obtained from Merck. PCL is an oil based biodegradable semicrystalline polymer with the linear formula $(C_6H_{10}O_2)_n$. Potassium phosphate buffer (PBS) 1 mM, was prepared in ultrapure water (obtained from Direct-Q™ 5 Ultrapure Water) and sterilized prior to use. Five fluorescent probes for the evaluation of specific physiological parameters were obtained from Thermo Fisher and applied for flow cytometry (FCM) analysis: 2′,7′-dichlorodihydrofluorescein diacetate (DCFH), dihydrorhodamine 123 (DHR 123), Bis-(1,3-dibutylbarbituric acid) trimethine oxonol (DiBAC$_4$(3)), 2′,7′-bis(2-carboxyethyl)-5(6)-carboxy fluorescein (BCECF), fluorescein diacetate (FDA). Specific information, concentration and incubation times are described in Table S1. All fluorochrome stock solutions were prepared in dimethyl sulfoxide and stored at −20 °C.

2.2. Abiotic degradation assay

In order to classify and study the PCL by-products during the degradation, the size typologies were defined based on (Hartmann et al., 2019): submicron-plastics (sMPs) and nanoplastics (NPs), defined as plastic particles with largest dimension in the 1 μm to 100 nm range and < 100 nm, respectively; additional PCL by-products obtained by ultrafiltration with 50 kDa (MWCO) filters are considered oligomers. PCL degradation assays were conducted by incubating 1 g of PCL beads in 20 mL of 1 mM PBS at pH 7 in 50 mL Erlenmeyer flasks, at 28 °C ± 2 on a rotary shaker at 135 rpm, under a light intensity of ~65 μmol photons m^2 s^{-1} (Philips Master TL-D 90 De Luxe 36 W/965) during 1, 2, 3, 5, 7, 14, 21, 31, 69, 100 and 132 days of abiotic degradation (all degradation assays were conducted in triplicate). In all samples at the specified time point, supernatants (without beads) were collected to assess the concentration of each class size of by-products released. The concentration of PCL by-products was calculated by measuring total organic carbon (TOC) and applying the ratio of C per PCL molecule (0.632 mg TOC/mg PCL). 8 mL of the supernatant were filtered twice through 100 nm sterile polyvinylidene difluoride (PVDF) syringe filters (Thermo Fisher) followed by TOC measurement to determine the concentration of all by-products < 100 nm (denoted as TOC_p in equations [1], [2]). Other 8 mL were filtered using 50 kDa (equivalent to ~ 5 nm regularly shaped particles (Erickson, 2009), hereinafter 5 nm) polyethersulfone Vivaspin 20 mL ultrafiltration tubes (Sartorius), previously washed following manufacturer's recommendation (first wash with 20 mL of hydrochloric acid 0.1 M and 3 more washes with 20 mL of ultrapure water). TOC in ultrafiltrates allowed determining the concentration of PCL oligomers smaller than 5 nm, denoted as TOC_g in equations [2], [3]. Beads were dried during 24 h at 37 °C and weighed to determine their total weight loss, denoted as T in equation (1). The amount of PCL for each size class was obtained as follows:

$$T- (TOC_p/0.632) = \text{mg/L of secondary sMPs } (>100 \text{ nm}) \quad [1]$$

$$TOC_p/0.632 – TOC_g/0.632 = \text{mg/L of secondary PCL-NPs (from 100 to} \sim 5 \text{ nm)} \quad [2]$$

$$TOC_g/0.632 = \text{mg/L of secondary PCL oligomers } (<5 \text{ nm}) \quad [3]$$

The remaining volume (4 mL) was used to assess NPs diameter and number using a Zetasizer Ultra from Malvern. The material < 100 nm released after 14 days (based on the results of the degradation studies with PS (Lambert and Wagner, 2016) and PCL (Kasuya et al., 1998) was vacuum dried for physicochemical characterization. Polymer identification was performed by micro-Fourier Transform Infrared Spectroscopy

(μFTIR) using a Perkin-Elmer Spotlight 200 Spectrum Two apparatus equipped with an MCT detector. This material was placed over potassium bromide discs. The equipment operated in transmission mode with 8 cm^{-1} resolution and spectral range 4000–550 cm^{-1}. Surface morphology was studied by scanning electron microscopy (SEM) using chromium-coated PCL beads and PCL-NPs previously dried on aluminum foils. Glass transition temperature (T_g) from the PCL-NPs powder was measured by differential scanning calorimetry (DSC). Polymeric chains length and structure (linear or cyclic) was assessed by mass spectrometry with MALDI-TOF/TOF configuration and NdYAG laser (355 nm) ULTRAFLEX III (Brunker Daltoniks GmbH, Bremen, Germany). MALDI TOF/TOF analyses were performed essentially as described by Storey et al., 2001 with some modifications, over the first 21 days of degradation. Briefly, vacuum dried samples were dissolved in tetrahydrofuran using 2,5-dihydroxybenzoic acid as matrix (10 mg/mL in methanol with 10% of water); the spectra was analyzed based on the PCL monomer molecular weight (114 Da) and type (linear or cyclic, what implies the presence or not of H_2O) as well as on the cation exchanged (Na^+ and K^+). The PCL-NPs + PCL oligomers suspension released after 14 days was directly used to measure hydrodynamic size by dynamic light scattering (DLS) and to determine surface net charge through the ζ-potential measured by electrophoretic light scattering (ELS) with a Zetasizer Nano ZS (Malvern).

2.3. Toxicity bioassays

The assays were conducted using two cyanobacteria: The filamentous heterocystous *Anabaena*, which fixes atmospheric nitrogen, and the unicellular *Synechococcus*. The cyanobacteria were routinely grown under light irradiation *ca.* 65 μmol photons m^2 s^{-1}, at 28 °C, on a rotary shaker (135 rpm) in 100 mL of culture media using 250 mL Erlenmeyer flasks for 3 days. *Anabaena* was grown in Allen & Arnon (A&A) culture medium diluted sixteen-fold and supplemented with nitrate (2.5 mM) (Allen and Arnon, 1955). *Synechococcus* was cultured in four-fold diluted BG11 medium (Rippka, 1988). Both cyanobacteria were acclimated to their corresponding culture medium. The hardness and conductivity of the culture media were similar to those found in rivers and effluents from wastewater treatment plants (Paredes et al., 2010; Perona et al., 1999; Singh et al., 2019). 20 g of PCL beads were incubated for 14 days in 200 mL of PBS (1 mM) and supernatants (without beads) were collected under the same conditions as described above. Next, half of the supernatant was filtered through 100 nm PVDF syringe filters (obtaining NPs together with oligomers, hereinafter the PCL-NPs + PCL oligomers fraction), and the other half was filtered using the 50 kDa MWCO ultrafiltration tubes to isolate the PCL oligomers fraction. *Anabaena* and *Synechococcus* were both exposed to the suspension containing the PCL-NPs

+ PCL oligomers and to the isolated PCL oligomers in order to assess the toxic action of these types of PCL degradation by-products. Fig. S1 represents the experimental set up scheme followed for the toxicological study in which both treatments are described: the exposure to all by-products < 100 nm, namely, PCL-NPs + PCL oligomers, and the exposure only to the by-products < 5 nm or 50 kDa denoted as PCL oligomers. The final volume for the bioassays was 10 mL (in 25 mL Erlenmeyer flasks) from which 1 mL was the appropriate culture medium (10-fold concentrated), 0.5 mL cell suspension (after growing 3 days, the cells were washed and concentrated with initial $OD_{750nm} = 0.15$), and the other 8.5 mL corresponded to the tested suspensions. Every treatment was conducted by triplicate under *ca.* 65 μmol photons m^2 s^{-1}, at 28 °C, on a rotary shaker (135 rpm) for 72 h. As controls for both treatments, cyanobacteria cultures with the same initial $OD_{750} = 0.15$, were exposed in the same way as described above by adding 8.5 mL of PBS (1 mM) or 8.5 mL of PBS filtered by 50 kDa MWCO ultrafiltration tubes. The growth of the cyanobacteria was assessed by chlorophyll *a* content (extraction was performed in 90% methanol for 24 h at 4 °C) measured spectrophotometrically at 665 nm after 24 and 72 h of exposure.

2.4. Physiological toxicity endpoints

The study of the mechanisms of toxic action of PCL by-products < 100 nm was performed by exposing both cyanobacteria to two independent treatments: PCL-NPs + PCL oligomers and PCL oligomers. The study was carried out by flow cytometry, by tracking photosynthesis (measuring oxygen evolution) and by analyzing heterocyst differentiation and nitrogenase activity of *Anabaena* under nitrogen deprivation conditions (using gas chromatography and confocal microscopy). In order to study morphological alterations on *Anabaena* and *Synechococcus*, 8 μL of exposed culture aliquots were dried over a glass slide to be observed directly by SEM. FCM analyses of *Anabaena* and *Synechococcus* cells were carried out on a FC500 Flow Cytometry Analyzer (Beckman Coulter) equipped with argon-ion excitation wavelength (488 nm), a detector of forward scatter (FS), a detector of side scatter (SS) and four fluorescence detectors with different wavelength intervals: 505–550 nm (FL1), 550–600 nm (FL2), 600–645 nm (FL3) and >645 nm (FL4). Seven physiological parameters were analyzed by FC; two of them, cell size and intracellular complexity, are correlated directly to the FCM output of FS and SS, respectively, and the other five were assessed using specific fluorochromes. Reactive oxygen species (ROS) overproduction was assessed using DCFH as general ROS formation indicator, while DHR 123 was used for hydrogen peroxide. Cytoplasmatic membrane potential was determined using $DiBAC_4(3)$, intracellular pH with BCECF, and unspecific esterase activity by means of FDA following the procedures described elsewhere (see Table S1) (Tamayo-Belda et

al., 2019). Data was collected using Kaluza software version 1.1 (Beckman Coulter). In order to investigate whether PCL by-products affect N_2 fixation, *Anabaena* was grown in the same conditions indicated above but with eight-fold diluted A&A without combined nitrogen and exposed to both PCL by-products treatments. Nitrogenase activity was determined by the acetylene reduction method and carried out as previously described (Mateo et al., 1986). Ethylene production was determined using a Shimadzu GC-8A gas chromatograph. The development of heterocyst after the first 24 h in the absence of nitrate was also studied by confocal microscopy using excitation laser set at 488 nm and the emission filter at 665 nm for photosynthetic pigments fluorescence as described by (Tamayo-Belda et al., 2021).

2.5. Data analysis

Mean and standard deviation values were calculated from at least three independent replicates by experiment. Significant differences between the treatments were calculated by one-way analysis of variance (ANOVA) with Dunnett's test using SigmaPlot 11.0. Software, considering statistically significant differences when $p < 0.05$.

3. Results and discussion

3.1. Physicochemical characterization of PCL degradation beads and fragments

The release of secondary plastic fragments from PCL beads was studied during 132 days of hydrolytic degradation. Firstly, the surface of the PCL beads was studied by SEM at time point zero and after 30, 69, 100 and 132 days to assess the morphological alterations following degradation. Fig. 1A revealed gradual smoothing of the surface, in agreement with observations reported elsewhere (González-Pleiter et al., 2019). During the first days of aging, the disappearance from the surface of several irregular structures (in the micron and sub-micron range) was clear, followed by a constant decrease of surface roughness. The chemical changes produced by hydrolytic degradation were tracked using μFTIR. Fig. 1B shows the μFTIR spectra of PCL beads for the same degradation periods showed for SEM. PCL beads at time zero (not degraded), displayed the characteristic peaks of PCL: 2949 cm^{-1} (asymmetric CH_2 stretching); 2865 cm^{-1} (symmetric CH_2 stretching); 1727 cm^{-1} (C=O stretching); 1293 cm^{-1} (C–O and C–C stretching in the crystalline phase) 1240 cm^{-1} (asymmetric COC stretching); 1190 cm^{-1} (OC–O stretching); 1170 cm^{-1}

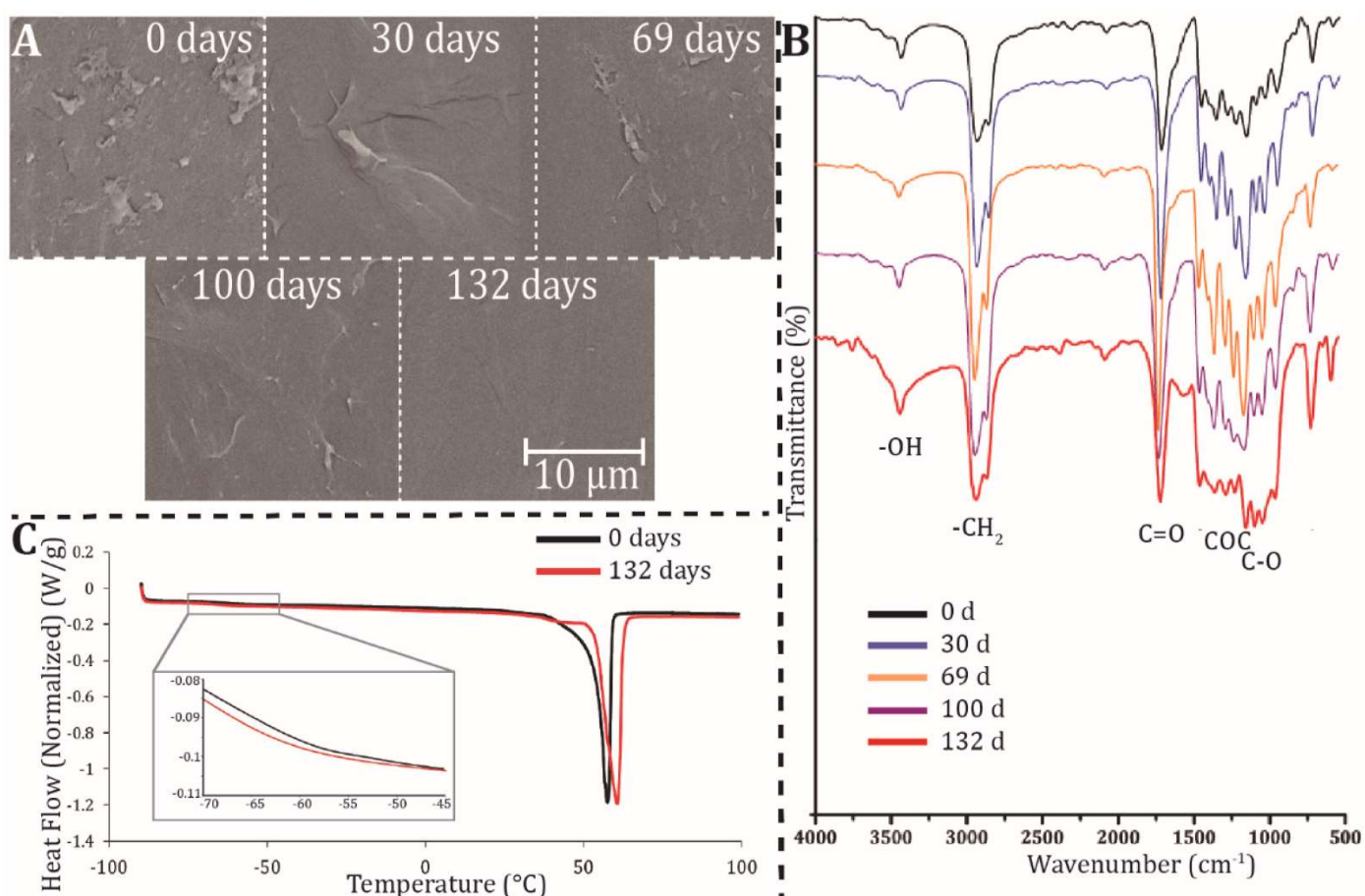**Figure 1**. Structural and chemical analysis of PCL beads during the degradation process in PBS (1 mM), at 28 °C, under light (~65 μmol photons m2 s−1) and shaking conditions. A) SEM images of PCL beads after 0–132 days. B) μFTIR spectra of PCL beads after 0–132 days. C) DSC spectra between −100 and 100 °C of PCL beads at 0 and 132 days of degradation (inset expand the spectra region where Tg is observed).

(symmetric COC stretching; and 1157 cm⁻¹ (C–O and C–C stretching in the amorphous phase) (Elzein et al., 2004). The main difference of the spectra of PCL beads after treatment was the peak at 1550 cm⁻¹, which clearly appeared after 132 days, which could be attributed to the carboxylate anions that appear at the end of some oligomers during the degradation of PCL (Bartnikowski et al., 2019; Oike et al., 1999; Ouhadi et al., 1976).

Since the hydrolytic degradation occurs primarily in the amorphous regions of the polymer, changes in the crystallinity of the bulk polymer are expected to occur (Lam et al., 2008). DSC thermograms of PCL beads showed a change in glass transition temperature (T_g) from -65.69 ± 0.29 to -66.14 ± 0.10 (Fig. 1C, inset). Melting temperature (T_m) increased gradually (Fig. S2) from 57.89 ± 0.27 to 60.05 ± 0.67 and, accordingly, crystallinity increased from ~55% to ~58% after 132 days (Fig. 1C).

The PCL by-products obtained in the concentration of PBS were classified by three different sizes (PCL sMPs, PCL-NPs and PCL oligomers) and quantified using TOC measurements. In Fig. 2, the concentration is expressed in terms of mg of PCL by-products per g of PCL beads (the release was also estimated by surface area considering the bead shape as an ellipsoid, based on the measured weight as well as the density and size displayed by the manufacturer Fig. S3). During the first 2–3 weeks there was an increase of the total by-products released, after which the rate subsequently decreased until the end of the exposure period. A similar observation was reported by Bartnikowski et al. (2019), where there is a rapid increase of the mass of released oligomers during the same period. Then it stabilizes around ~3 mg of PCL oligomer/g of PCL bead probably due to a deceleration of bulk degradation. Kasuya et al. (1998) also reported this after two weeks of PCL degradation in natural river water. This deceleration probably co-occurred with an aggregation process between the PCL oligomers and the particulate fractions; thus, part of the PCL oligomers would be removed from the water column by ultrafiltration, resulting in a reduction of TOC measurement (Wahl et al., 2021). NPs release increased during the first 2 days and stabilized thereafter at ~1 mg of PCL-NPs/g of PCL bead. The release of NPs could be related to the degradation of amorphous regions revealed by the observed increase in crystallinity (Fig. 1C) and the absence of crystallinity in the PCL-NPs + PCL oligomers sample (Fig. S4). Accordingly, the degradation of PCL would be accompanied by the formation of a NPs-rich phase in the surrounding medium. The particulate fraction > 100 nm was within the 100–1000 nm range after 132 days (Fig. S5) so this fraction was considered as sMPs, which was found to be present during the whole degradation time.

In order to confirm the release of nanometric fragments, SEM images were taken from vacuum dried PCL-NPs + PCL oligomers samples released after 14 days of degradation. As shown in Fig. 3A.1, a large number of particles in the nanometric range were observed. We checked the possibility that the observed nanostructures could be crystals generated during vacuum drying. However, crystals displayed cubic and regular shapes (Fig. S6), easily distinguishable from the irregular morphologies of the NPs (which were clearly observed at higher magnifications) (Fig. 3A.2). In addition, we found irregular aggregates of 200–300 nm (Fig. 3A.3). The chemical nature of the nanometric particles was confirmed by µFTIR spectrum (Fig. 3B) that displayed the same specific peaks of PCL previously observed with the PCL beads. Including the one at 1550 associated to the presence of carboxylate anions, that was only observed in the bulk polymer after 132 days (Fig. 1B). Thus, we could unambiguously assess the release of secondary PCL-NPs during the abiotic degradation of PCL, as previously reported for other oil-based polymers (Lambert and Wagner, 2016) as well as for biodegradable polymers (González-Pleiter et al., 2019). Non-Invasive Back-Scatter optics (NIBS®), Multi-Angle Dynamic Light Scattering (MADLS®) and DLS were used to track the size distribution and particle concentration of the PCL-NPs released (Fig. 3C and D, respectively). The concentration of PCL-NPs was in the 10^9-10^{11} particles g⁻¹ range. Remarkably, during the first days in PBS, the release of particles reached a maximum (~4–6 × 10^{10} particles g⁻¹) to decrease and thereafter stabilize. After 2 months of degradation, a slightly increase in terms of mass was observed (Fig. 2). This might be related to mass changes in the other size typologies; and to the release of the most exposed crystalline domains due to the degradation of the surrounding amorphous regions as proposed by Lam et al. (2008). Therefore, since the first day in PBS, a nano-size plastic phase clearly appeared.
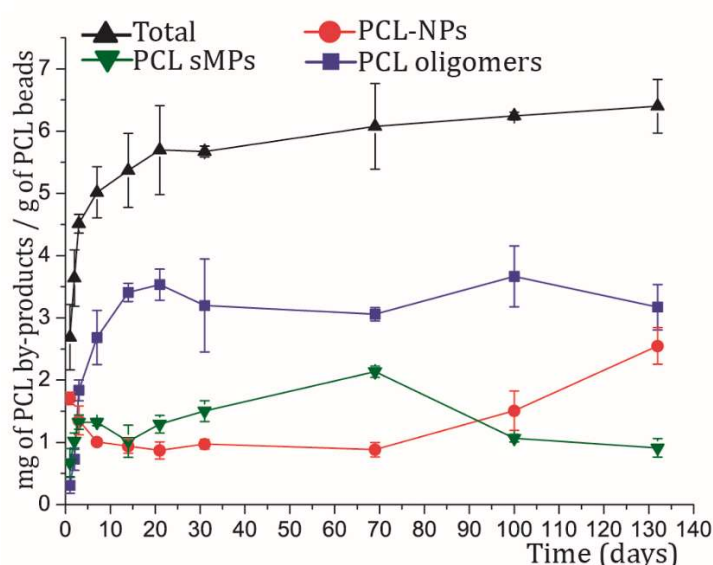

Figure 2. Mass of PCL fragments from the three size classes measured by TOC and weight loss released over 132 days of PCL beads degradation in PBS (results are represented as average ± SD of 3 independent replicates).
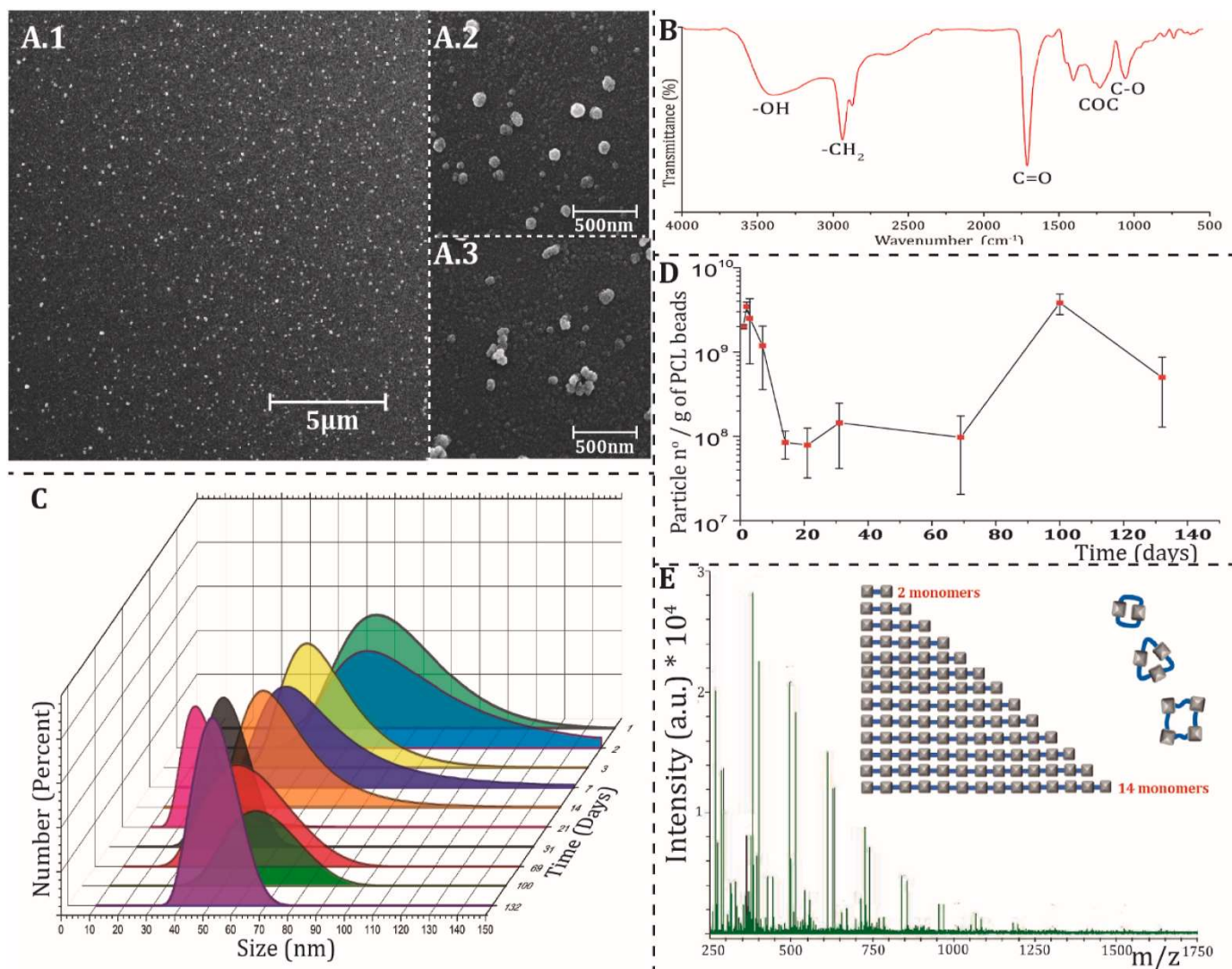
Figure 3. Fragmentation of PCL beads from 0 to 132 days in PBS (1 mM), at 28 °C, under light (~65 μmol photons m^2 s^{-1}) and shaking. A.1) SEM images of the PCL-NPs + PCL oligomers fractions released after 14 days of degradation. A.2) and A.3) Higher magnification SEM image of dispersed and aggregated PCL-NPs, respectively. B) μFTIR spectra of PCL-NPs + PCL oligomers fraction released after 14 days of degradation. C) Size distribution of the PCL-NPs + PCL oligomers* fractions as a function of degradation time. D) Particle number of PCL-NPs + PCL oligomers* released throughout the 132 days of degradation. E) MALDI mass spectra of the PCL-NPs + PCL oligomers fraction released after 14 days. (* The oligomeric fraction was not detected by DLS techniques.)

Additionally, ELS result indicated negative surface charge of the particles after 14 days, with a ζ-potential of −24.9 ± 3.6 mV at pH 7, indicating a stable colloidal suspension as previously reported for other secondary nanoplastics (El Hadri et al., 2020; González-Pleiter et al., 2019).

MALDI-TOF/TOF was applied to assess the polymeric chain type and length of PCL-NPs and oligomers released after 14 days of degradation in PBS. Fig. 3E shows the following peaks: linear polymer $[(C_6H_{10}O_2)_nH_2O]Na^+$: 269-383-497-611-725 … 1639 and $[(C_6H_{10}O_2)_nH_2O]K^+$: 285-399-513-627-741 … 1653 (n = from 2 to 14 monomers); cyclic polymer $[(C_6H_{10}O_2)_n]Na^+$: 251-365-479 and $[(C_6H_{10}O_2)_n]K^+$: 267-381-495 (n = from 2 to 4 monomers). The results showed cyclic and linear chains up to 14 units length (~1600 Da). These were slightly larger than those reported by (Bosworth and Downes, 2010) after 90 days of degradation of PCL scaffolds (similar chain

length was observed over the first 21 days of degradation Fig. S7). Furthermore, the observed release of PCL oligomers was consistent with the small reduction (6–7%) of the molecular weight of PCL scaffolds observed by Lam et al. (2009) after 12 months in PBS. Therefore, we confirmed the release of PCL-NPs and PCL oligomers from PCL beads in different concentrations over 132 days of degradation in PBS. The molecular structure of these by-products probably consists of less organized and low molecular weight polymeric chains. As a summary, in Fig. 4 we propose a degradation scheme of PCL during its hydrolytic degradation.

Our results showed that even at early degradation states, hydrolysis and chain scission led to the release of high amount of PCL-NPs and PCL oligomers. PCL oligomers consisted of short linear and cyclic polymeric chains of hundreds-to-few thousands Da (Fig. 3E). PCL-NPs are probably being released from amorphous

regions given that hydrolysis occurs mainly there, which causes an overall increase in crystallinity (Fig, S3). After a few days, PCL-NPs release slowed down whilst the PCL oligomer concentration in the surrounding PBS increased for 2–3 more weeks. After two months, the presence of isolated crystalline regions could be involved on the slight variation of particulate fractions (PCL-NPs and sub-MPs) concentration. After approximately 4 months of degradation a concentration of about 2 mg of PCL-NPs per g of PCL beads still remained in suspension.
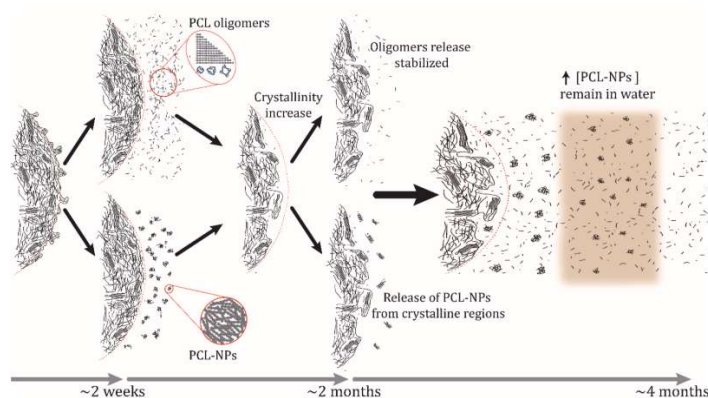
Figure 4. Proposed scheme for PCL hydrolytic degradation.

3.2. Effects of hydrolytic degradation PCL by-products < 100 nm to cyanobacteria

The threat posed by the presence of the smallest fractions of plastics in aquatic ecosystems has been widely explored during the last decade (Baudrimont et al., 2019; Besseling et al., 2014; Booth et al., 2016; Cao et al., 2021; Chae et al., 2018; Feng et al., 2019; Sjollema et al., 2016; Venâncio et al., 2021).

Nevertheless, a limited number of studies have addressed the toxicity of those coming from biodegradable plastics, the materials expected to replace traditional oil-based plastics for a wide variety of applications (Green et al., 2016, 2021; Palsikowski et al., 2018; Yokota and Mehlrose, 2020; Zhang et al., 2021; Zhuikov et al., 2021; Zimmermann et al., 2020). To our knowledge, there is only one previous study that tested secondary NPs from a biodegradable polymer (González-Pleiter et al., 2019), but there is a complete lack of studies regarding the toxicity of PCL by-products in aquatic environments. In the present work, two aquatic cyanobacteria, one filamentous heterocystous N_2-fixing (*Anabaena*) and one unicellular (*Synechococcus*) have been used to assess the toxicity of PCL by-products released during 14-days degradation. The toxicity was tested for different sizes: by-products < 100 nm, namely, secondary PCL-NPs + PCL-oligomers fraction as well as the PCL oligomers fraction alone. According to TOC measurements, both cyanobacteria were exposed to 91 mg/L and 238 mg/L of PCL-NPs and PCL oligomers, respectively. As shown in Fig. 5, cell growth, expressed as chlorophyll *a* content, both cyanobacteria were affected when exposed to a combination of PCL-NPs + PCL oligomers after 24 and 72 h.

Interestingly, after removing the particulate material by ultrafiltration, the exposure of only the PCL oligomers resulted in considerably lower toxicity than when exposed to the PLC-NPs. In *Synechococcus* this produced a significant growth decrease after 72 h. The filamentous cyanobacterium, *Anabaena*, was clearly less affected than the unicellular *Synechococcus*, which showed more sensitivity to both treatments. In order to
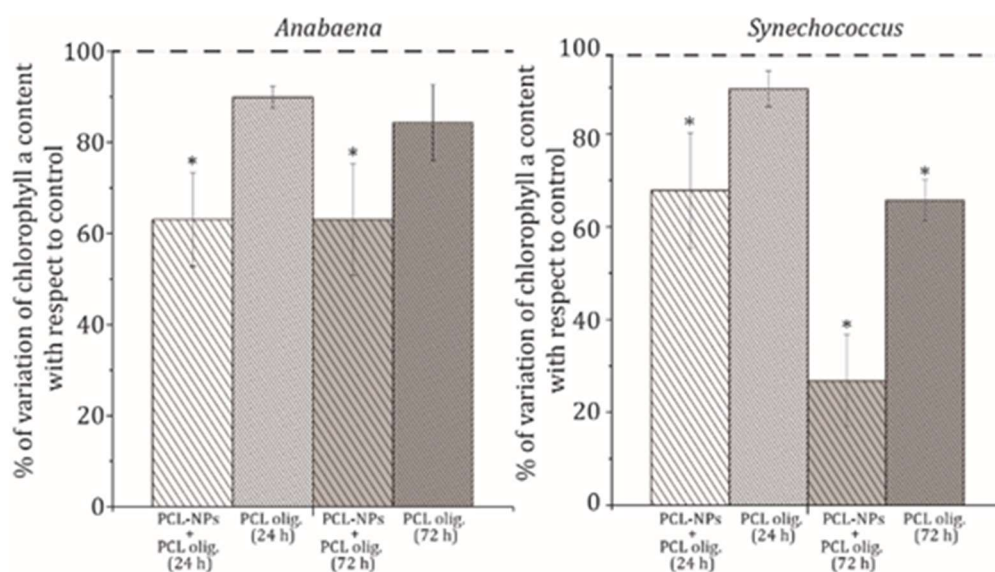

Figure 5. Effect of PCL-NPs + PCL oligomers and PCL oligomers (released after 14 days of PCL degradation) on the growth (assessed by chlorophyll a content) of both cyanobacteria after 24 and 72 h of exposure. 14 days aged PBS and 14 days aged, and filtered PBS (50 kDa ultrafiltration tubes) were used for the non-exposed controls of PCL-NPs + PCL oligomers and PCL oligomers, respectively. Asterisks indicate treatments that are significantly different from the control (p < 0.05, Dunnett's test). Fig. S8 shows representative graphics from where these results were obtained.
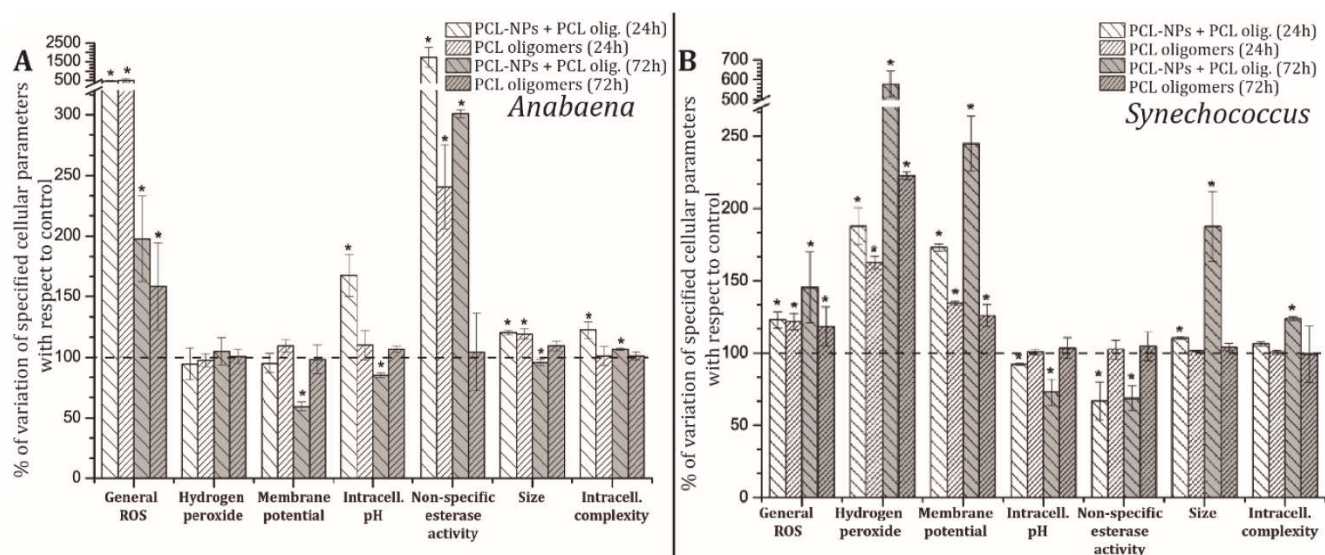
Figure 6. Effect of PCL-NPs + PCL oligomers and PCL oligomers (released after 14 days of PCL degradation) on several physiological parameters expressed as variation ± SD with respect to the control in Anabaena and *Synechococcus* after 72 h of exposure. 14 days aged PBS and 14 days aged, and filtered PBS (50 kDa ultrafiltration tubes) were used for the non-exposed controls of PCL-NPs + PCL oligomers and PCL oligomers, respectively. Asterisks indicate treatments that are significantly different from the control (p < 0.05, Dunnett's test). Fig. S9 and S10 show representative graphics from where these results were obtained.

study the physiological changes induced by the PCL by-products exposure, five different fluorescent probes were used in FMC analyses to track the status of relevant physiological parameters that could be potentially altered upon exposure. Fig. 6 shows the effects that the exposure to both PCL-NPs + PCL oligomers and PCL oligomers caused on *Anabaena and Synechococcus*, respectively.

Significant <u>ROS</u> overproduction (based on general ROS) was observed in *Anabaena*. There were no significant differences for the ROS response in *Anabaena* between PCL-NPs + PCL oligomers and PCL oligomers exposure. However, in both cases ROS production significantly decreased from 24 to 72 h of exposure; no H_2O_2 production was observed, meaning that other ROS might be involved. In *Synechococcus*, general ROS also increased significantly after exposure to both fractions and a clear H_2O_2 overproduction was observed. Interestingly such increase was lower when the cyanobacterium was exposed only to PCL oligomers. In cyanobacteria, as photosynthetic organisms, oxidative stress is a consequence of the exposure to toxics due to the fragile equilibrium of their redox homeostasis (Gonzalo et al., 2015; Hurtado-Gallego et al., 2020; Latifi et al., 2009; Tamayo-Belda et al., 2021). ROS overproduction has also been described together with the alteration in membrane potential on microalgae exposed to nanoparticles (Hurtado-Gallego et al., 2020; Martín-De-Lucía et al., 2018; Pulido-Reyes et al., 2019; Tamayo-Belda et al., 2019). In the present study, when *Anabaena* was exposed to PCL-NPs + PCL oligomers a decrease of DiBAC4(3) fluorescence was observed only after 72 h which indicated some degree of membrane hyperpolarization. Membrane hyperpolarization has

already been observed in the cyanobacterium *Microcystis aeruginosa* upon exposure to the antibiotics erythromycin and sulfamethoxazole at lower concentrations than those that induced membrane depolarization (Schon et al., 1990; Seoane et al., 2017a, 2017b; Zhang et al., 2020); it is usually attributed to the impairment of the proton pump or the alteration of normal ion permeability. When tested only in the presence of PCL oligomers it did not result in altered membrane potential. On the contrary, *Synechococcus* exposed to both PCL-NPs + PCL oligomers underwent a clear membrane depolarization (fluorescence increase) after 24 and 72 h (~150% and ~250% respectively, with respect to the controls), which indicated severe membrane alteration with loss of membrane potential (Pikula et al., 2019; Rioboo et al., 2009). This indicates that the unicellular cyanobacterium is more sensitive than *Anabaena* to this fraction of PCL by-products. The exposure of only PCL oligomers provoked a membrane depolarization significantly lower (about 130% at 24 and 72 h, with respect to the control). These results suggest that PCL-NPs may be the main responsible of membrane alteration, probably due to physical abrasion (Morandi et al., 2021; Rossi et al., 2014; Tamayo-Belda et al., 2021), since the PCL oligomers alone barely triggered membrane damage in both cyanobacteria. Regarding intracellular pH, when *Anabaena* was in presence of PCL-NPs + PCL oligomers it suffered an intracellular alkalinization (increase in the fluorescent intensity of BCECF) after 24 h followed by an acidification (decrease in fluorescent intensity) after 72 h. The alkalinization may be a consequence of the consumption of intracellular protons by the reactions involved in ROS metabolism, an outcome that has been previously related to oxidative stress in algae (Cid et

al., 2013; Gonzalez-Pleiter et al., 2017). The acidification observed after 72 h in *Anabaena,* and after both 24 and 72 h in *Synechococcus*, has been previously associated to the loss of membrane integrity or deficient proton pump activity (Feng et al., 2019; Tamayo-Belda et al., 2019, 2021). Metabolic activity was studied by evaluating the non-specific esterase activity. Results were in line with the lower sensitivity of *Anabaena,* whose metabolism increases probably as an attempt to face the toxicity triggered by PCL by-products (Rioboo et al., 2009). The higher toxicity observed for *Synechococcus* was in accordance with the clear decrease in metabolic activity. When exposed only to PCL oligomers, in general, the non-specific esterase activity values are similar to those of the controls supporting the hypothesis that the main toxic effects are produced by PCL-NPs. Regarding structural damages, shortened filaments and swollen cells were observed upon PCL-NPs + PCL oligomers exposure, accompanied by an increase of internal complexity (Fig. 6). Both effects have been previously observed as consequence of nanoparticles exposure (Gonzalo et al., 2015; Pandey et al., 2012; Shirazi et al., 2015; Tamayo-Belda et al., 2019); interestingly, morphological alterations were not induced when exposing cells only to the oligomers fraction (Fig. S11). Accordingly, the so far described cellular damages could be mostly attributed to the released secondary PCL-NPs.

Cyanobacteria are among the few organisms on earth capable of performing nitrogen fixation under aerobic conditions; in particular, *Anabaena* presents specialized cells called heterocysts. They are surrounded by thick cell walls, which create a nearly anaerobic intracellular milieu so that nitrogenase activity is not inactivated by oxygen (Mateo et al., 2015; Wolk, 1998; Wood and Haselkorn, 1980). We studied the heterocyst differentiation and nitrogen fixation (nitrogenase activity) of *Anabaena* exposed to PCL-NPs + PCL oligomers and to PCL oligomers alone. Confocal microscopy was used to check for patterned loss of red fluorescence. This occurs due to the degradation of phycobiliproteins at an early stage of heterocyst development (Wolk, 1998; Wood and Haselkorn, 1980). As shown in Fig. 7A, after 24 h under nitrogen deprivation conditions, controls were able to develop mature heterocysts. Both PCL-NPs + PCL oligomers and PCL oligomers exposures hampered heterocyst differentiation. The cells pointed by arrows seem to be proheterocysts or immature heterocysts (still with autofluorescence of the photosynthetic pigments), which indicates an abnormal developmental pattern or an arrest in cell differentiation (Kumar et al., 2010; Torrecilla et al., 2004). In both cases, nitrogenase activity was strongly affected, being reduced up to 20% of control values (Fig. 7B).
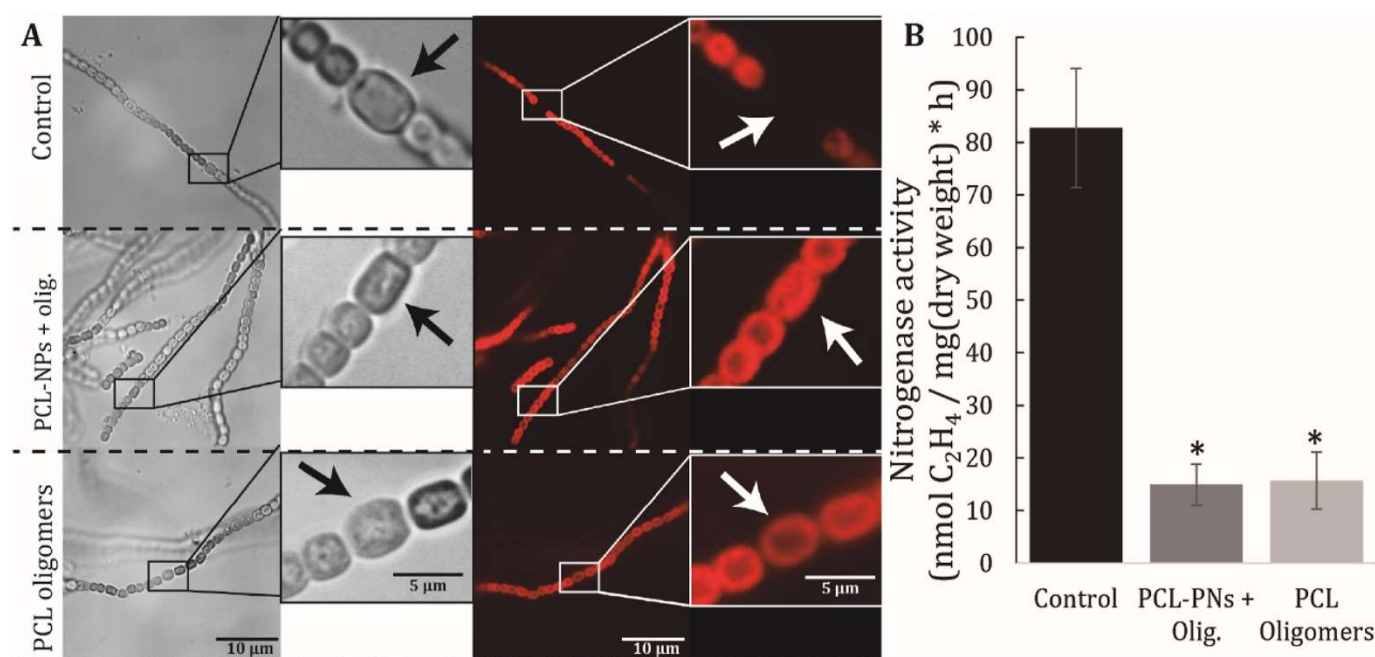

Figure 7. valuation of nitrogen fixation related parameters. A) Effect on heterocyst development of *Anabaena* (arrows indicate heterocysts after 24 h of nitrogen deprivation). B) Effects on nitrogenase activity of *Anabaena*. Asterisks indicate treatments that are significantly different from the control (p < 0.05, Dunnett's test).

The decrease of nitrogen fixation rate has been previously described for cyanobacteria exposed to nanoparticles as well as to organic pollutants. Mishra and Pandey (1989) studied the effects of some common rice field herbicides, such as 2,4-dichlorophenoxyacetic acid (2,4-D), Machete, and Saturn, on paddy field nitrogen-fixing cyanobacteria *Nostoc linckia*, *Nostoc calcicola*, *Nostoc* sp., and *Anabaena doliolum*. Interestingly, 2,4-D stimulated the growth and nitrogen fixation at concentrations above those used in the rice fields. Machete and Saturn, however, did not stimulate nitrogen fixation or growth even at lower

concentrations. Cherchi and Gu (2010) investigated the impact of titanium dioxide nanomaterials (nTiO2) exposure on cell growth, nitrogen fixation activity, and nitrogen storage dynamics in the cyanobacterium *Anabaena variabilis*. They found that the nitrogen fixation activity was severely impacted by nTiO2, implying that nitrogen fixation might be hampered by the release of nTiO2 in aquatic environments. Huang et al. (2020) investigated the effect of silver nanoparticles (AgNPs) on photosynthesis and nitrogen fixation of the cyanobacterium *Nostoc sphaeroides*. The authors found that only high doses of AgNPs (1 mg/L) caused growth inhibition, reactive oxygen species overproduction and decreased N_2 fixation.

This is the first time that this effect is described upon exposure to plastic degradation by-products, it is a very interesting result as both PCL-NPs, and PCL oligomers significantly impaired nitrogen fixation in *Anabaena*.

4. Conclusions

Under environmentally representative conditions secondary PCL-NPs, as well as sMPs and oligomers were released from PCL beads by abiotic degradation. Considerable amount of PCL-NPs and PCL oligomers were measured over 4 months. Results indicated that the presence of PCL plastics in water might imply the presence of a continuous concentration of secondary nanoplastics and oligomers in the water column that could be considered as "pseudo-persistent" pollutants. Both PCL-NPs and PCL oligomers, but largely the nanoparticulate fraction, were harmful for two photosynthetic organisms that play a key role in freshwater ecosystems. In particular, both PCL-degradation fractions inhibited nitrogen fixation in *Anabaena* by arresting heterocyst differentiation. This may be clearly detrimental for the aquatic organisms as N_2 fixation by free-living cyanobacteria is an important way of entry of N into the trophic chain. It is clear from this study that fragmentation of a bioplastic may render a continuous production of secondary nanoplastics as well as oligomers that might be toxic to the surrounding biota. Thus efforts should be made to thoroughly understand the fragmentation of plastics, including the so-considered safer bioplastics, and the toxicity of the smallest size fractions resulting from that degradation.

References

Abriata, J.P., Turatti, R.C., Luiz, M.T., Raspantini, G.L., Tofani, L.B., do Amaral, R.L.F., Swiech, K., Marcato, P.D., Marchetti, J.M., 2019. Development, characterization and biological in vitro assays of paclitaxel-loaded PCL polymeric nanoparticles. Mater. Sci. Eng. C 96, 347–355.

Agarwal, S., 2020. Biodegradable polymers: present opportunities and challenges in providing a microplastic-free environment. Macromol. Chem. Phys. 221, 6, 2000017.

Al Hosni, A.S., Pittman, J.K., Robson, G.D., 2019. Microbial degradation of four biodegradable polymers in soil and compost demonstrating polycaprolactone as an ideal compostable plastic. Waste Manage. 97, 105–114.

Ali Akbari Ghavimi, S., Ebrahimzadeh, M.H., Solati-Hashjin, M., Abu Osman, N.A., 2015. Polycaprolactone/starch composite: fabrication, structure, properties, and applications. J. Biomed. Mater. Res. 103, 2482–2498.

Allen, M.B., Arnon, D.I., 1955. Studies on nitrogen-fixing blue-green algae. Plant Physiol. 30 (4), 366–372.

Azimi, B., Nourpanah, P., Rabiee, M., Arbab, S., 2014. Poly (ε-caprolactone) fiber: an overview. J. Eng. Fiber. Fabr. 9, 74–90.

Bartnikowski, M., Dargaville, T.R., Ivanovski, S., Hutmacher, D.W., 2019. Degradation mechanisms of polycaprolactone in the context of chemistry, geometry and environment. Prog. Polym. Sci. 96, 1–20.

Baudrimont, M., Arini, A., Gu′egan, C., Venel, Z., Gigault, J., Pedrono, B., Prunier, J., Maurice, L., Halle, A. Ter, Feurtet-mazel, A., 2019. Ecotoxicity of polyethylene nanoplastics from the North Atlantic oceanic gyre on freshwater and marine organisms (microalgae and filter-feeding bivalves). Environ. Sci. Pollut. Res. 27, 3746–3755.

Besseling, E., Wang, B., Lu, M., Koelmans, A.A., 2014. Nanoplastic A ff ects Growth of S. obliquus and Reproduction of D. magna. Environ. Sci. Technol. 48, 12336–12343.

Booth, A.M., Hansen, B.H., Frenzel, M., Johnsen, H., Altin, D., 2016. Uptake and toxicity of methylmethacrylate-based nanoplastic particles in aquatic organisms. Environ. Toxicol. Chem. 35, 1641–1649.

Bosworth, L.A., Downes, S., 2010. Physicochemical characterisation of degrading polycaprolactone scaffolds. Polym. Degrad. Stabil. 95, 2269–2276.

Cao, J., Liao, Y., Yang, W., Jiang, X., Li, M., 2021. Enhanced microalgal toxicity due to polystyrene nanoplastics and cadmium co-exposure: from the perspective of physiological and metabolomic profiles. J. Hazard Mater. 427, 127937.

Cesari, A., Loureiro, M.V., Vale, M., Yslas, E.I., Dardanelli, M., Marques, A.C., 2020. Polycaprolactone microcapsules containing citric acid and naringin for plant growth and sustainable agriculture: physico-chemical properties and release behavior. Sci. Total Environ. 703, 135548.

Chae, Y., Kim, D., Kim, S.W., An, Y.J., 2018. Trophic transfer and individual impact of nano-sized polystyrene in a four-species freshwater food chain. Sci. Rep. 8, 1–11.

Chamas, A., Moon, H., Zheng, J., Qiu, Y., Tabassum, T., Jang, J.H., Abuomar, M., Scott, S.L., Suh, S., 2020. Degradation rates of plastics in the environment. ACS Sustain. Chem. Eng. 8, 3494–3511.

Cherchi, C., Gu, A.Z., 2010. Impact of titanium dioxide nanomaterials on nitrogen fixation rate and intracellular nitrogen storage in Anabaena variabilis. Environ. Sci. Technol. 44, 8302–8307.

Cid, A., Prado, R., Rioboo, C., Suárez-Bregua, P., Herrero, C., 2013. Use of microalgae as biological indicators of pollution: looking for new relevant cytotoxicity endpoints. Microalgae Biotechnol. Microbiol. Energy 311–324.

Degli-Innocenti, F., 2014. Biodegradation of plastics and ecotoxicity testing: when should it be done. Front. Microbiol. 5, 1–3.

Diyanat, M., Saeidian, H., Baziar, S., Mirjafary, Z., 2019. Preparation and characterization of polycaprolactone nanocapsules containing pretilachlor as a herbicide nanocarrier. Environ. Sci. Pollut. Res. 26, 21579–21588.

El Hadri, H., Gigault, J., Maxit, B., Grassl, B., Reynaud, S., 2020. Nanoplastic from mechanically degraded primary and secondary microplastics for environmental assessments. NanoImpact 17, 100206.

Elzein, T., Nasser-Eddine, M., Delaite, C., Bistac, S., Dumas, P., 2004. FTIR study of polycaprolactone chain organization at interfaces. J. Colloid Interface Sci. 273, 381–387.

Erickson, H.P., 2009. Size and shape of protein molecules at the nanometer level determined by sedimentation, gel filtration, and electron microscopy. Biol. Proced. Online 11, 32–51.

Eriksen, M., Lebreton, L.C.M., Carson, H.S., Thiel, M., Moore, C.J., Borerro, J.C., Galgani, F., Ryan, P.G., Reisser, J., 2014. Plastic pollution in the World's oceans: more than 5 trillion plastic pieces weighing over 250,000 tons afloat at sea. PLoS One 9 (12), 1–15.

European Bioplastics, 2021. Bioplastics Materials. https://www.european-bioplastics.org/market/ (Accessed 17 February 2022).

Feng, L., Li, J., Xu, E.G., Sun, X., Zhu, F., Ding, Z., Tian, H., Dong, S., Xia, P., Yuan, X., 2019. Short-term exposure to positively charged polystyrene nanoparticles causes oxidative stress and membrane destruction in cyanobacteria. Environ. Sci. Nano 6, 3072–3079.

Geyer, R., 2020. Production, Use, and Fate of Synthetic Polymers, Plastic Waste and Recycling. Academic Press, 13-22.

González-Pleiter, M., Rioboo, C., Reguera, M., Abreu, I., Leganés, F., Cid, A., Fernández-Piñas, F., 2017. Calcium mediates the cellular response of Chlamydomonas reinhardtii to the emerging aquatic pollutant Triclosan. Aquat. Toxicol. 186, 50–66.

González-Pleiter, M., Tamayo-Belda, M., Pulido-Reyes, G., Amariei, G., Leganés, F., Rosal, R., Fernández-Piñas, F., 2019. Secondary nanoplastics released from a biodegradable microplastic severely impact freshwater environments. Environ. Sci. Nano 6, 1382–1392.

Gonzalo, S., Rodea-Palomares, I., Leganés, F., García-Calvo, E., Rosal, R., Fernández-Piñas, F., 2015. First evidences of PAMAM dendrimer internalization in microorganisms of environmental relevance: a linkage with toxicity and oxidative stress. Nanotoxicology 9, 706–718.

Green, D.S., Boots, B., O'Connor, N.E., Thompson, R., 2016. Microplastics affect the ecological functioning of an important biogenic habitat. Environ. Sci. Technol. 51, 68–77.

Green, D.S., Jefferson, M., Boots, B., Stone, L., 2021. All that glitters is litter? Ecological impacts of conventional versus biodegradable glitter in a freshwater habitat. J. Hazard Mater. 402, 124070.

Groh, K.J., Backhaus, T., Carney-almroth, B., Geueke, B., Inostroza, P.A., Lennquist, A., Leslie, H.A., Maf, M., Slunge, D., Trasande, L., Warhurst, A.M., Muncke, J., 2019. Science of the Total Environment Overview of Known Plastic Packaging-Associated Chemicals and Their Hazards 651, pp. 3253–3268.

Hartmann, N.B., Hu, T., Thompson, R.C., Hassello, M., Verschoor, A., Daugaard, A.E., Rist, S., Karlsson, T., Brennholt, N., Cole, M., Herrling, M.P., Hess, M.C., Ivleva, N.P., Lusher, A.L., Wagner, M., 2019. Are We speaking the same language? recommendations for a definition and categorization framework for plastic debris. Environ. Sci. Technol. 53, 1039–1047.

Havstad, M.R., 1994. Biodegradable plastics. Nippon Nogeikagaku Kaishi 68 (9), 1318–1320.

Huang, M., Keller, A.A., Wang, X., Tian, L., Wu, B., Ji, R., Zhao, L., 2020. Low concentrations of silver nanoparticles and silver ions perturb the antioxidant defense system and nitrogen metabolism in N_2-fixing cyanobacteria. Environ. Sci. Technol. 54, 15996–16005.

Huang, J., Shew, A.S., Wang, M., 1990. Biodegradable plastics: a review. Adv. Polym. Technol. 1, 23–30.

Hurtado-Gallego, J., Pulido-Reyes, G., González-Pleiter, M., Salas, G., Leganés, F., Rosal, R., Fernández-Piñas, F., 2020. Toxicity of superparamagnetic iron oxide nanoparticles to the microalga *Chlamydomonas Reinhardtii*, vol. 238, pp. 2–11.

Iñiguez, M.E., Conesa, J.A., Fullana, A., 2017. Microplastics in Spanish table salt. Sci. Rep. 7, 1–7.

Irizar, A., Amorim, M.J.B., Fuller, K.P., Zeugolis, D.I., Scott-Fordsmand, J.J., 2018. Environmental fate and effect of biodegradable electro-spun scaffolds (biomaterial)-A case study. J. Mater. Sci. Mater. Med. 29, 51.

Jarrett, P., Benedict, C.V., Bell, J.P., Cameron, J.A., Huang, S.J., 1984. In: Shalaby, S.W., Hoffman, A.S., Ratner, B.D., Horbett, T.A. (Eds.), Polymers as Biomaterials, Springer. 181–192.

Kasuya, K.I., Takagi, K.I., Ishiwatari, S.I., Yoshida, Y., Doi, Y., 1998. Biodegradabilities of various aliphatic polyesters in natural waters. Polym. Degrad. Stabil. 59, 327–332.

Krasowska, K., Heimowska, A., Morawska, M., 2016. Environmental degradability of polycaprolactone under natural conditions. E3S Web Conf. 10, 00048.

Kumar, K., Mella-Herrera, R.A., Golden, J.W., 2010. Cyanobacterial heterocysts. Cold Spring Harbor Perspect. Biol. 2/4/a000315.

Lam, C.X.F., Hutmacher, D.W., Schantz, J.T., Woodruff, M.A., Teoh, S.H., 2009. Evaluation of polycaprolactone scaffold degradation for 6 months in vitro and in vivo. J. Biomed. Mater. Res. 90, 906–919.

Lam, C.X.F., Savalani, M.M., Teoh, S.H., Hutmacher, D.W., 2008. Dynamics of in vitro polymer degradation of polycaprolactone-based scaffolds: accelerated versus simulated physiological conditions. Biomed. Mater. 3, 0341083.

Lambert, S., Wagner, M., 2016. Characterisation of nanoplastics during the degradation of polystyrene. Chemosphere 145, 265–268.

Latifi, A., Ruiz, M., Zhang, C.C., 2009. Oxidative stress in cyanobacteria. FEMS Microbiol. Rev. 33, 258–278.

Lewis, S.L., Maslin, M.A., 1964. Defining the Anthropocene. Nature 519, 171–180.

Martín-De-Lucía, I., Campos-Mañas, M.C., Agüera, A., Leganés, F., Fernández-Piñas, F., Rosal, R., 2018. Combined toxicity of graphene oxide and wastewater to the green alga *Chlamydomonas reinhardtii*. Environ. Sci. Nano 5, 1729–1744.

Mateo, P., Bonilla, I., Fernández-Valiente, E., Sánchez-Maeso, E., 1986. Essentiality of boron for dinitrogen fixation in *Anabaena* sp. PCC 7119. Plant Physiol. 81, 430–433.

Mateo, P., Leganés, F., Perona, E., Loza, V., Fernández-Piñas, F., 2015. Cyanobacteria as bioindicators and bioreporters of environmental analysis in aquatic ecosystems. Biodivers. Conserv. 24, 909–948.

Mattsson, K., Jocic, S., Doverbratt, I., Hansson, L., 2018. Nanoplastics in the aquatic environment. In: Microplastic Contamination in Aquatic Environments. Elsevier Inc., pp. 379–399.

Mishra, A.K., Pandey, A.B., 1989. Toxicity of three herbicides to some nitrogen-fixing cyanobacteria. Ecotoxicol. Environ. Saf. 17, 236–246.

Morandi, M.I., Kluzek, M., Wolff, J., Schroder, A., Thalmann, F., Marques, C.M., 2021. Accumulation of styrene oligomers alters lipid membrane phase order and miscibility. Proc. Natl. Acad. Sci. 118, 1–7.

Narancic, T., Cerrone, F., Beagan, N., O'Connor, K.E., 2020. Recent advances in bioplastics: application and biodegradation. Polymers 12, 4, 920.

Obayashi, T., Kinoshita, K., 2009. Rank of correlation coefficient as a comparable measure for biological. Signific. Gene Coexpression 16, 249–260.

Oike, H., Imamura, H., Imaizumi, H., Tezuka, Y., 1999. Tailored synthesis of branched and network polymer structures by electrostatic self-assembly and covalent fixation with telechelic poly(THF) having AT-phenylpyrrolidinium salt groups. Macromolecules 32, 4819–4825.

Ouhadi, T., Stevens, C., Teyssi´e, P., 1976. Study of poly-ε-caprolactone bulk degradation. J. Appl. Polym. Sci. 20, 2963–2970.

Palsikowski, P.A., Roberto, M.M., Sommaggio, L.R.D., Souza, P.M.S., Morales, A.R., Marin-Morales, M.A., 2018. Ecotoxicity evaluation of the biodegradable polymers PLA, PBAT and its blends using Allium cepa as test organism. J. Polym. Environ. 26, 938–945.

Pandey, S., Rai, R., Rai, L.C., 2012. Proteomics combines morphological, physiological and biochemical attributes to unravel the survival strategy of *Anabaena* sp. PCC7120 under arsenic stress. J. Proteonomics 75, 921–937.

Paredes, J., Andreu, J., Solera, A., 2010. A decision support system for water quality issues in the Manzanares River (Madrid, Spain). Sci. Total Environ. 408, 2576–2589.

Perona, E., Bonilla, I., Mateo, P., 1999. Spatial and temporal changes in water quality in a Spanish river. Sci. Total Environ. 241, 75–90.

Persenaire, O., Alexandre, M., Degée, P., Dubois, P., 2001. Mechanisms and kinetics of thermal degradation of poly(ε-caprolactone). Biomacromolecules 2, 288–294.

Picó, Y., Barceló, D., 2019. Analysis and prevention of microplastics pollution in water: Current perspectives and future directions. ACS Omega 4, 6709–6719.

Pikula, K.S., Chernyshev, V.V., Zakharenko, A.M., Chaika, V.V., Waissi, G., Hai, L.H., Hien, T.T., Tsatsakis, A.M., Golokhvast, K.S., 2019. Toxicity assessment of particulate matter emitted from different types of vehicles on marine microalgae. Environ. Res. 179, 108785.

Pouladchang, A., Tavanai, H., Morshed, M., Khajehali, J., Shamsabadi, A.S., 2022. Controlled release of thiram pesticide from polycaprolactone micro and nanofibrous mat matrix. J. Appl. Polym. Sci. 139, 51641.

Pulido-Reyes, G., Briffa, S.M., Hurtado-Gallego, J., Yudina, T., Leganés, F., Puntes, V., Valsami-Jones, E., Rosal, R., Fernández-Piñas, F., 2019. Internalization and toxicological mechanisms of uncoated and PVP-coated cerium oxide nanoparticles in the freshwater alga *Chlamydomonas reinhardtii*. Environ. Sci. Nano 6, 1959–1972.

Pulido-Reyes, G., Rodea-Palomares, I., Das, S., Sakthivel, T.S., Leganes, F., Rosal, R., Seal, S., Fernandez-Piñas, F., 2015. Untangling the biological effects of cerium oxide nanoparticles: the role of surface valence states. Sci. Rep. 5, 15613.

Raina, N., Pahwa, R., Khosla, J.K., Gupta, P.N., Gupta, M., 2021. Polycaprolactone-based materials in wound healing applications. Polym. Bull. 1-23.

RameshKumar, S., Shaiju, P., O'Connor, K.E., P, R.B., 2020. Bio-based and biodegradable polymers - state-of-the-art, challenges and emerging trends. Curr. Opin. Green Sustain. Chem. 21, 75–81.

Rioboo, C., Prado, R., Herrero, C., Cid, ́A., 2009. Cytotoxic effects of pesticides on microalgae determined by flow cytometry. Repos. Univ. Coruña. http://hdl.handle.net/2183/16609.

Rippka, R., 1988. Isolation and purification of cyanobacteria. Methods Enzymol 167, 3–27.

Rivas, D., Ginebreda, A., Pérez, S., Quero, C., Barcel ́o, D., 2016. MALDI-TOF MS Imaging evidences spatial differences in the degradation of solid polycaprolactone diol in water under aerobic and denitrifying conditions. Sci. Total Environ. 566–567, 27–33.

Rossi, G., Barnoud, J., Monticelli, L., 2014. Polystyrene nanoparticles perturb lipid membranes. J. Phys. Chem. Lett. Lett. 5, 241–246.

Schon, M.K., Novacky, A., Blevins, D.G., 1990. Boron induces hyperpolarization of sunflower root cell membranes and increases membrane permeability to K+. Plant Physiol. 93, 566–571.

Seoane, M., Esperanza, M., Cid, A., 2017a. Cytotoxic effects of the proton pump inhibitor omeprazole on the non-target marine microalga *Tetraselmis suecica*. Aquat. Toxicol. 191, 62–72.

Seoane, M., Esperanza, M., Rioboo, C., Herrero, C., Cid, A., 2017b. Flow cytometric assay to assess short-term effects of personal care products on the marine microalga *Tetraselmis suecica*. Chemosphere 171, 339–347.

Shen, M., Song, B., Zeng, G., Zhang, Y., Huang, W., Wen, X., Tang, W., 2020. Are biodegradable plastics a promising solution to solve the global plastic pollution? Environ. Pollut. 263, 114469.

Shirazi, M.A., Shariati, F., Keshavarz, A.K., Ramezanpour, Z., 2015. Toxic effect of aluminum oxide nanoparticles on green micro-algae *Dunaliella salina*. Int. J. Environ. Res. 9, 585–594.

Singh, N., Tiwari, E., Khandelwal, N., Darbha, G.K., 2019. Understanding the stability of nanoplastics in aqueous environments: effect of ionic strength, temperature, dissolved organic matter, clay, and heavy metals. Environ. Sci. Nano 6, 2968–2976.

Sjollema, S.B., Redondo-hasselerharm, P., Leslie, H.A., Kraak, M.H.S., Vethaak, A.D., 2016. Do plastic particles affect microalgal photosynthesis and growth. Aquat. Toxicol. 170, 259–261.

Song, R., Murphy, M., Li, C., Ting, K., Soo, C., Zheng, Z., 2018. Current development of biodegradable polymeric materials for biomedical applications. Drug Des. Dev. Ther. 12, 3117–3145.

Storey, R.F., Brister, L.B., Sherman, J.W., 2001. Structural characterization of poly(ε-caprolactone) and poly(ε-caprolactone-b-isobutylene-b-ε-caprolactone) block copolymers by MALDI-TOF mass spectrometry. J. Macromol. Sci. Pure Appl. Chem. 38 A, 107-122.

Tamayo-Belda, M., González-Pleiter, M., Pulido-Reyes, G., Martin-Betancor, K., Leganés, F., Rosal, R., Fernández-Piñas, F., 2019. Mechanism of the toxic action of cationic G5 and G7 PAMAM dendrimers in the cyanobacterium *Anabaena* sp. PCC7120 Environ. Sci. Nano 6, 863–878.

Tamayo-Belda, M., Vargas-Guerrero, J.J., Martín-Betancor, K., Pulido-Reyes, G., González-Pleiter, M., Leganés, F., Rosal, R., Fernández-Piñas, F., 2021. Understanding nanoplastic toxicity and their interaction with engineered cationic nanopolymers in microalgae by physiological and proteomic approaches. Environ. Sci. Nano 8, 2277–2296.

Torrecilla, I., Leganés, F., Bonilla, I., Fernández-Piñas, F., 2004. A calcium signal is involved in heterocyst differentiation in the cyanobacterium *Anabaena* sp. PCC7120. Microbiology 150, 3731–3739.

Venâncio, C., Savuca, A., Oliveira, M., Martins, M.A., Lopes, I., 2021. Polymethylmethacrylate nanoplastics effects on the freshwater cnidarian *Hydra viridissima*. J. Hazard Mater. 402, 123773.

Wahl, A., Le Juge, C., Davranche, M., El Hadri, H., Grassl, B., Reynaud, S., Gigault, J., 2021. Nanoplastic occurrence in a soil amended with plastic debris. Chemosphere 262, 127784.

Wolk, P.C., 1998. Heterocyst formation in Anabaena. Curr. Opin. Microbiol. 1, 623–629.

Wood, N.B., Haselkorn, R., 1980. Control of phycobiliprotein proteolysis and heterocyst differentiation in *Anabaena*. J. Bacteriol. 141, 1375–1385.

Woodward, S.C., Brewer, P.S., Moatamed, F., Schindler, A., Pitt, C.G., 1985. The intracellular degradation of poly(ε-caprolactone). J. Biomed. Mater. Res. 19, 437–444.

Yokota, K., Mehlrose, M., 2020. Lake phytoplankton assemblage altered by irregularly shaped PLA body wash microplastics but not by PS calibration beads, Water, 12, 2650.

Zhang, Q., Qu, Q., Lu, T., Ke, M., Zhu, Y., Zhang, M., Zhang, Z., Du, B., Pan, X., Sun, L., Qian, H., 2018. The combined toxicity effect of nanoplastics and glyphosate on *Microcystis aeruginosa* growth. Environ. Pollut. J. 243, 1106–1112.

Zhang, M., Steinman, A.D., Xue, Q., Zhao, Y., Xu, Y., Xie, L., 2020. Effects of erythromycin and sulfamethoxazole on *Microcystis aeruginosa*: cytotoxic endpoints, production and release of microcystin-LR. J. Hazard Mater. 399, 123021.

Zhang, X., Xia, M., Su, X., Yuan, P., Li, X., Zhou, C., Wan, Z., Zou, W., 2021. Photolytic degradation elevated the toxicity of polylactic acid microplastics to developing zebrafish by triggering mitochondrial dysfunction and apoptosis. J. Hazard Mater. 413, 125321.

Zhuikov, V.A., Akoulina, E.A., Chesnokova, D.V., Wenhao, Y., Makhina, T.K., Demyanova, I.V., Zhuikova, Y.V., Voinova, V.V., Belishev, N.V., Surmenev, R.A., Surmeneva, M.A., Bonartseva, G.A., Shaitan, K.V., Bonartsev, A.P., 2021. The growth of 3t3 fibroblasts on PHB, PLA and PHB/PLA blend films at different stages of their biodegradation in vitro. Polymers 13, 1-23.

Zimmermann, L., Dombrowski, A., Völker, C., Wagner, M., 2020. Are bioplastics and plant-based materials safer than conventional plastics? In vitro toxicity and chemical composition. Environ. Int. 145, 106066.

SUPPLEMENTARY MATERIAL

Identification and toxicity towards aquatic primary producers of the smallest fractions released from hydrolytic degradation of polycaprolactone microplastics

MiguelT amayo-Belda[1], Gerardo Pulido-Reyes[1], Miguel González-Pleiter[1], Keila Martín-Betancor[1], Francisco Leganés[1], Roberto Rosal[2], FranciscaFernández-Piñas[1,*]

[1] Department of Biology, Faculty of Science, Universidad Autónoma de Madrid, E-28049, Madrid, Spain

[2] Department of Chemical Engineering, Universidad de Alcalá, 28805 Alcalá de Henares, Madrid, Spain

* Corresponding author: francisca.pina@uam.es

Contents:

Table S1. Concentrations and incubation times of the fluorochrome probes used for flow cytometry studies.

Fluorochrome	Acronym	Physiological parameter	Final concentration ($\mu g\ mL^{-1}$)	Incubation time (min)
2',7'-dichlorodihydrofluorescein diacetate	DCFH	General level of intracellular reactive oxygen species	100	30
Dihydrorhodamine 123	DHR123	Intracellular levels of hydrogen peroxide	10	40
Bis-(1,3-dibutylbarbituric acid) trimethine oxonol	DiBAC$_4$(3)	Cytoplasmic membrane potential	2.5	10
2',7'-bis(2-carboxyethyl)-5(6)-carboxy fluorescein	BCECF	Intracellular pH	5	40
Fluorescein Diacetate	FDA	Non-specific esterase activity	2.5	15
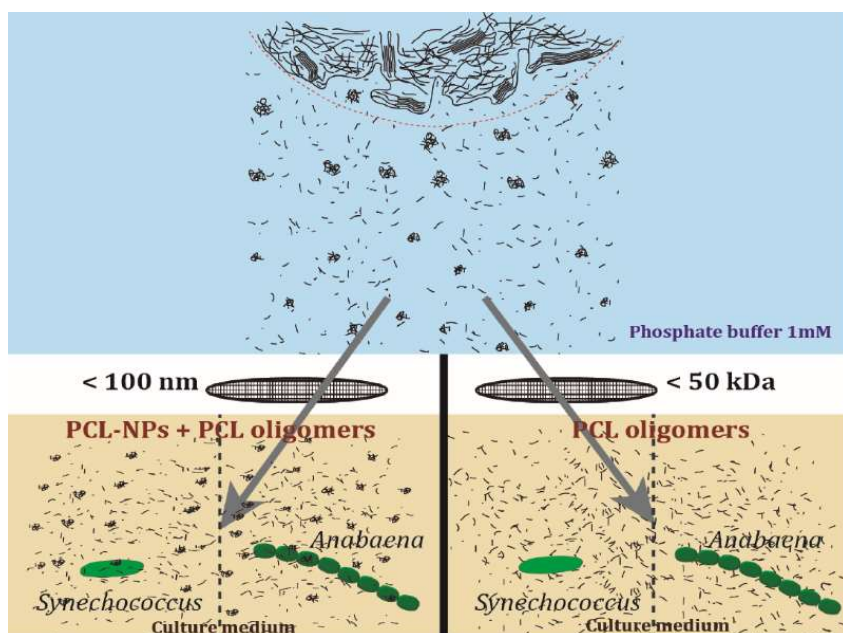
Figure S1. Scheme of the experimental set up design to study the toxicity of the fractions of PCL-NPs + PCL oligomers and of PCL oligomers released after 14 days of PCL degradation.
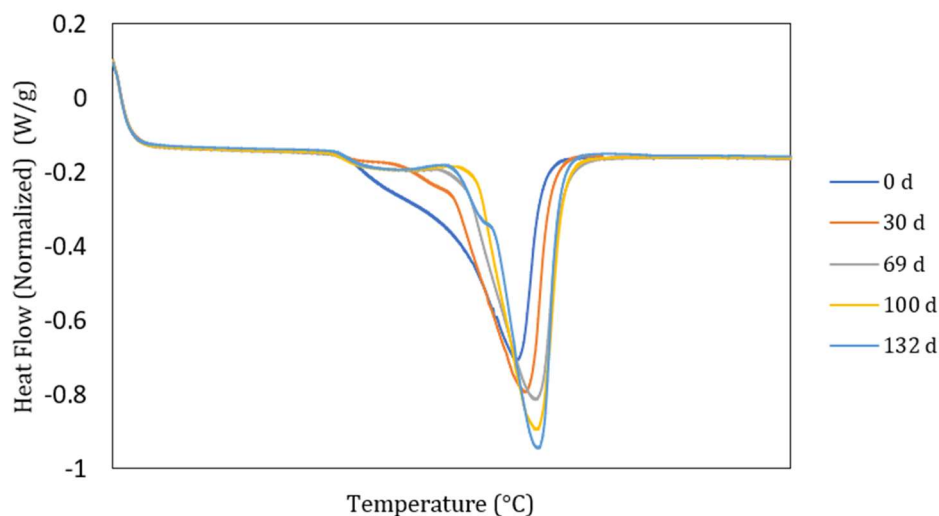
Figure S2. DSC of the PCL beads degraded in PBS up to 132 days.
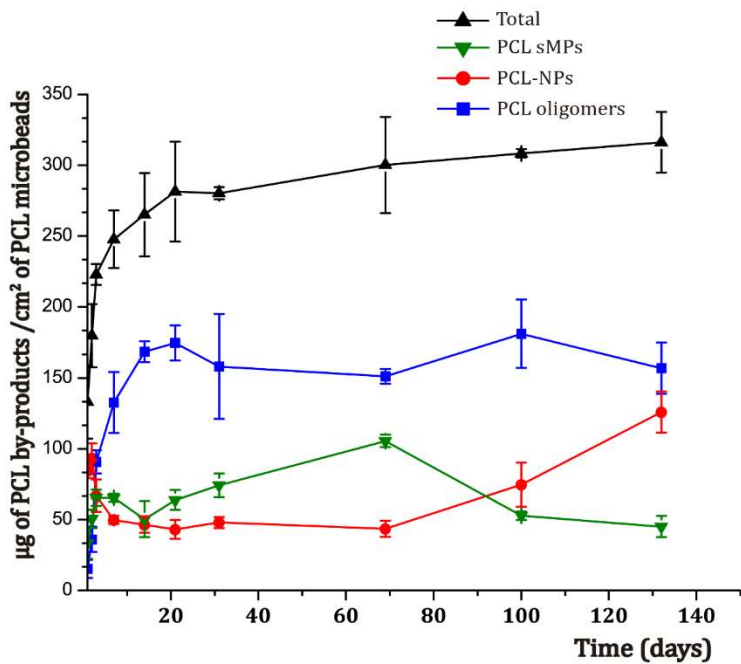
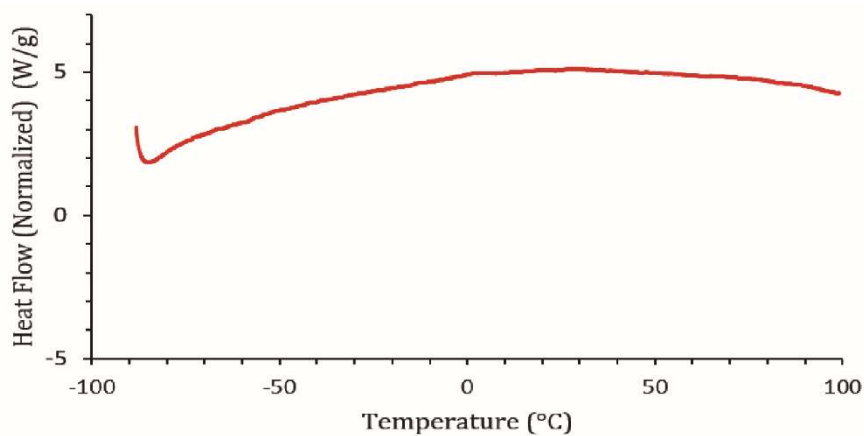**Figure S3**. PCL by-products by size classes released per unit surface of PCL beads.

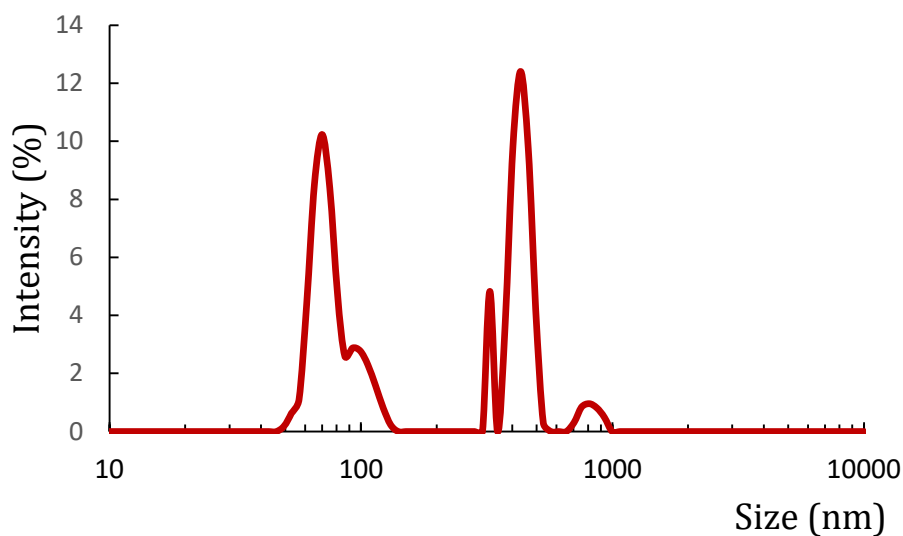**Figure S4**. DSC of the PCL-NPs + PCL oligomers degraded in PBS up to 14 days.

Figure S5. Size distribution of PCL particulate by-products (not filtered) after 132 days of degradation in PBS measured by Multi-Angle Dynamic Light Scattering (mean of 3 independent replicates).
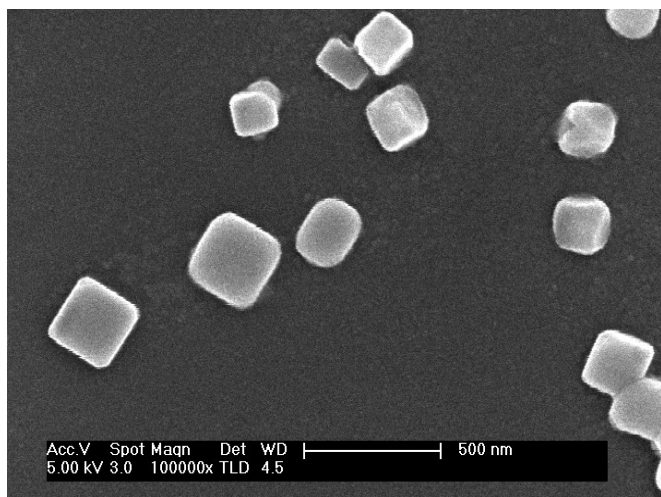
Chemosphere, 303, 134966, 2022

Figure S6. SEM images of crystals appeared after vacuum drying of PCL-NPs.
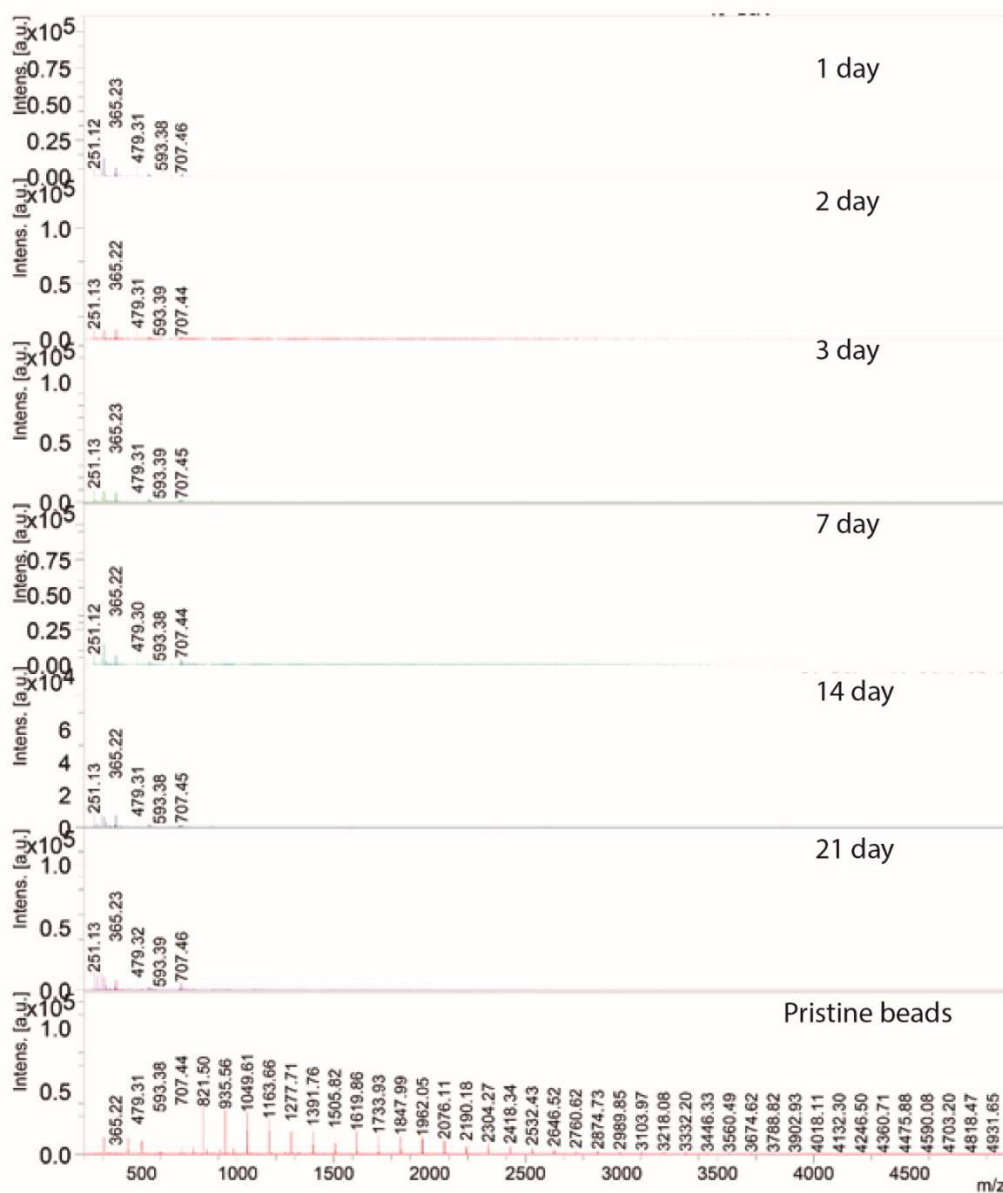
Figure S7. MALDI mass spectra of the PCL-NPs + PCL oligomers from 1 to 21 days of degradation and spectra of pristine beads.
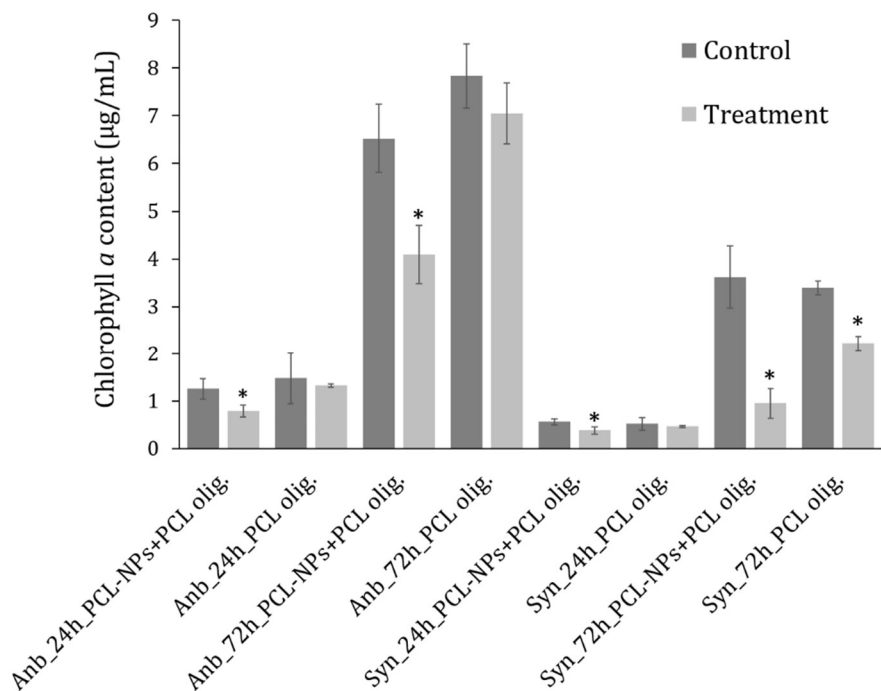
Figure S8. Effects of PCL-NPs + PCL oligomers and PCL oligomers (released after 14 days of PCL degradation) on the growth (assessed by chlorophyll a content) of *Anabaena* sp. PCC 7120 (Anb) and *Synechococcus* sp. PCC 7942 (Syn) after 24 and 72 h of exposure. 14 days aged PBS and 14 days aged and filtered PBS (50 KDa ultrafiltration tubes) were used for the non-exposed controls of PCL-NPs + PCL oligomers and PCL oligomers, respectively. Asterisks indicate treatments that are significantly different from the control ($p < 0.05$, Dunnett's test).
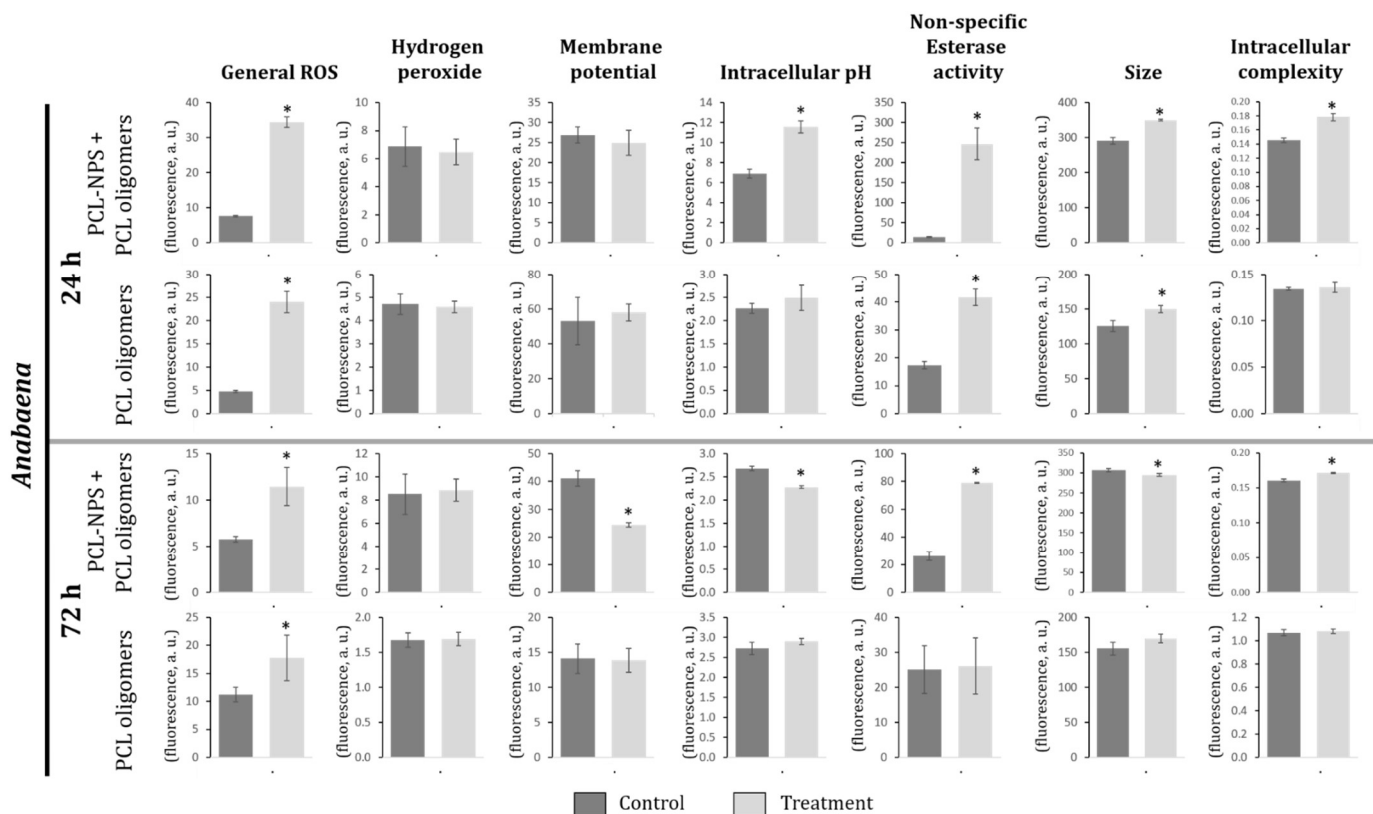

Figure S9. Effect of PCL-NPs + PCL oligomers and PCL oligomers (released after 14 days of PCL degradation) on several physiological parameters studied by flow cytometry and expressed as the mean of fluorescence arbitrary units (a.u.) ± SD in Anabaena after 72h of exposure. 14 days aged PBS and 14 days aged and filtered PBS (50 KDa ultrafiltration tubes) were used for the non-exposed controls of PCL-NPs + PCL oligomers and PCL oligomers, respectively. Asterisks indicate treatments that are significantly different from the control ($p < 0.05$, Dunnett's test).
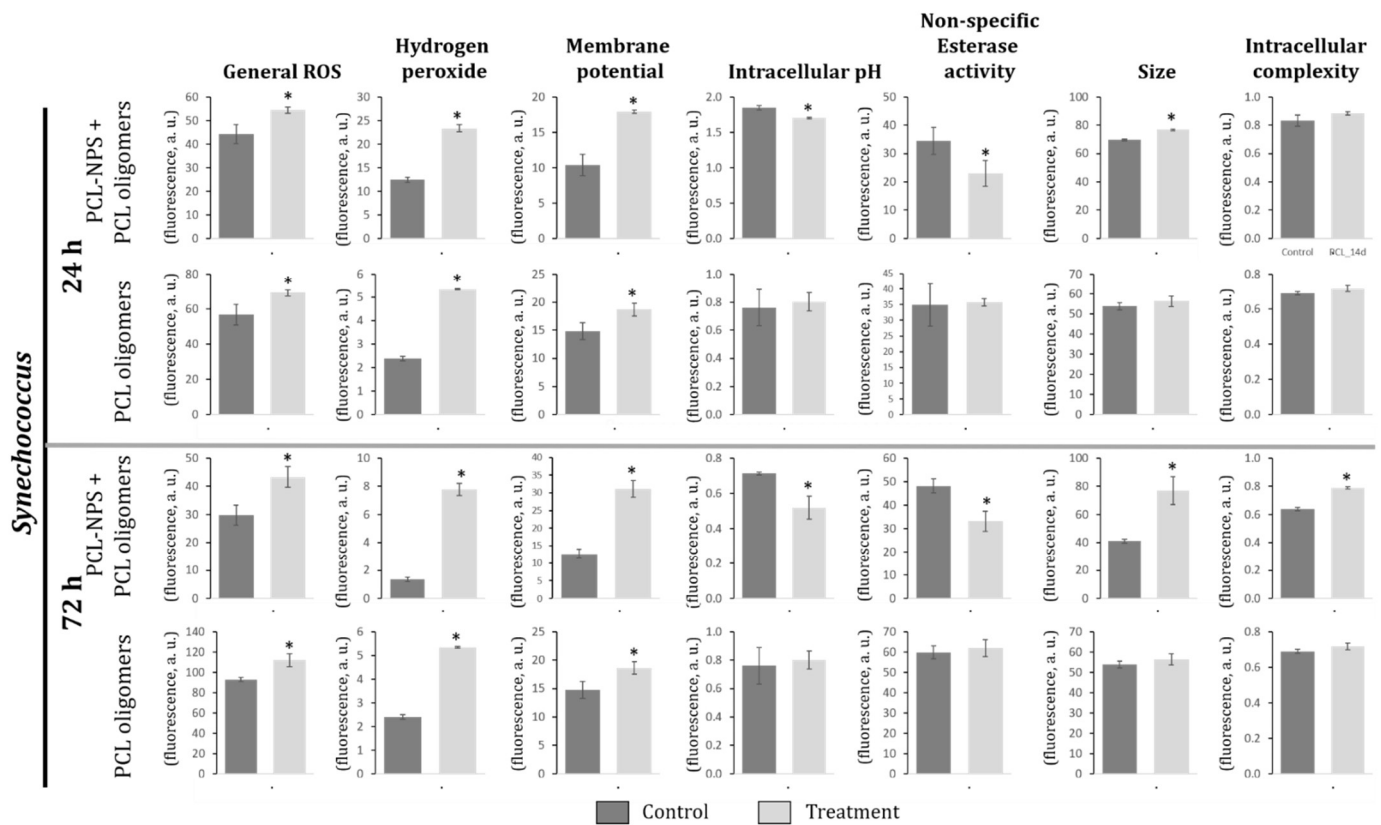
Figure S10. Effect of PCL-NPs + PCL oligomers and PCL oligomers (released after 14 days of PCL degradation) on several physiological parameters studied by flow cytometry and expressed as the mean of fluorescence arbitrary units (a.u.) ± SD in Synechococcus after 72h of exposure. 14 days aged PBS and 14 days aged and filtered PBS (50 KDa ultrafiltration tubes) were used for the non-exposed controls of PCL-NPs + PCL oligomers and PCL oligomers, respectively. Asterisks indicate treatments that are significantly different from the control (p < 0.05, Dunnett's test).
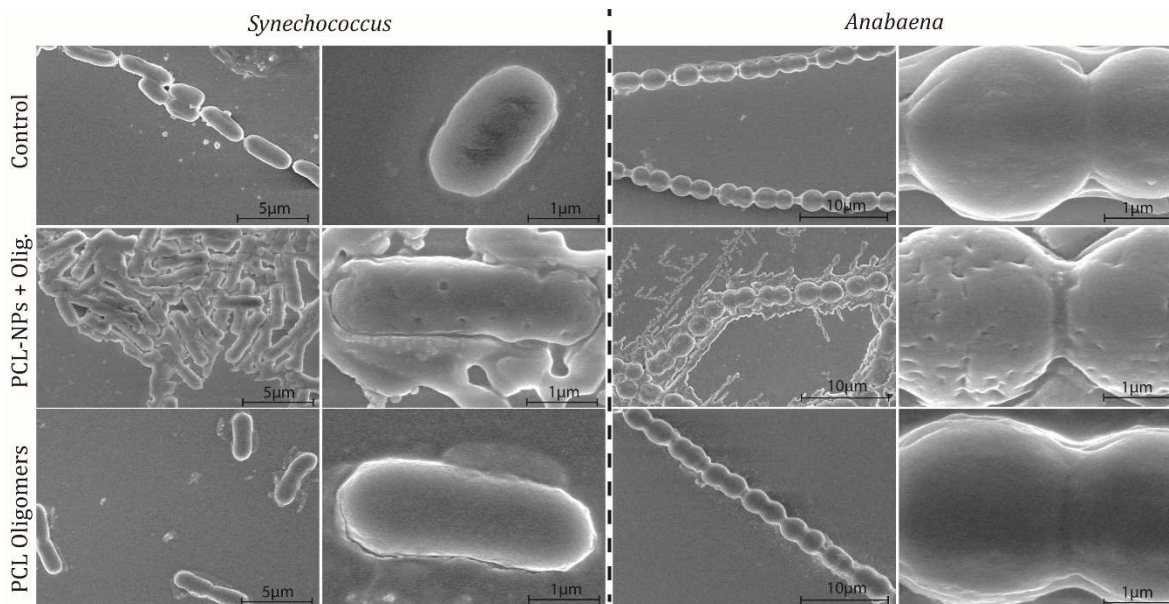

Figure S11. SEM images of *Synechococcus* and *Anabaena* exposed for 72 h to PCL-NPs + PCL oligomers and PCL oligomers only.